

VCBART: Bayesian trees for varying coefficients

Sameer K. Deshpande*, Ray Bai†, Cecilia Balocchi‡, Jennifer E. Starling§, Jordan Weiss¶

October 25, 2023

Abstract

The linear varying coefficient models posits a linear relationship between an outcome and covariates in which the covariate effects are modeled as functions of additional effect modifiers. Despite a long history of study and use in statistics and econometrics, state-of-the-art varying coefficient modeling methods cannot accommodate multivariate effect modifiers without imposing restrictive functional form assumptions or involving computationally intensive hyperparameter tuning. In response, we introduce VCBART, which flexibly estimates the covariate effect in a varying coefficient model using Bayesian Additive Regression Trees. With simple default settings, VCBART outperforms existing varying coefficient methods in terms of covariate effect estimation, uncertainty quantification, and outcome prediction. We illustrate the utility of VCBART with two case studies: one examining how the association between later-life cognition and measures of socioeconomic position vary with respect to age and socio-demographics and another estimating how temporal trends in urban crime vary at the neighborhood level. An R package implementing VCBART is available at <https://github.com/skdeshpande91/VCBART>.

*Department of Statistics, University of Wisconsin–Madison. sameer.deshpande@wisc.edu

†Department of Statistics, University of South Carolina

‡School of Mathematics, University of Edinburgh

§Mathematica Inc.

¶Stanford University

1 Introduction

1.1 Motivation

The linear varying coefficient model specifies a linear relationship between an outcome Y and p covariates X_1, \dots, X_p that is allowed to change according to the values of R *effect modifiers* Z_1, \dots, Z_R . That is, the model asserts that

$$Y = \beta_0(\mathbf{Z}) + \beta_1(\mathbf{Z})X_1 + \dots + \beta_p(\mathbf{Z})X_p + \varepsilon, \quad (1)$$

where the $\beta_0(\mathbf{Z}), \dots, \beta_p(\mathbf{Z})$ are *functions* mapping \mathbb{R}^R to \mathbb{R} and the residual error ε has mean zero. In this paper, we use Bayesian Additive Regression Trees (BART; [Chipman et al., 2010](#)) to learn the covariate effect functions $\beta_j(\mathbf{Z})$, expressing each with an ensemble of binary regression trees. Our proposed method, which we call VCBART, can produce extremely accurate estimates and well-calibrated uncertainty intervals of evaluations $\beta_j(\mathbf{z})$ and predictions $\mathbb{E}[Y|\mathbf{X} = \mathbf{x}, \mathbf{Z} = \mathbf{z}]$ without imposing rigid parametric assumptions or requiring computationally intensive tuning. VCBART further enjoys strong theoretical guarantees and scales gracefully to large datasets with tens of thousands of observations. The following applications motivate our work.

Socioeconomic position and cognition. A large body of evidence suggests that socioeconomic position (SEP) at different points in the life course is an important determinant of cognitive function in mid-life and older adulthood ([Luo and Waite, 2005](#); [Lyu and Burr, 2016](#); [Marden et al., 2017](#); [Greenfield and Moorman, 2019](#); [Zhang et al., 2020](#)). A critical open challenge in life course research involves estimating how the associations between cognition and various SEP measures evolve over time and with respect to sociodemographic characteristics. Typically, authors related cognitive outcome to several SEP variables with linear models that included pre-specified interactions between the SEP covariates and characteristics like age, gender, and race. For instance, both [Lyu and Burr \(2016\)](#) and [Marden et al. \(2017\)](#) modeled an interaction between SEP and age while [Aartsen et al. \(2019\)](#) introduced an additional interaction with age-squared. In doing so, these authors implicitly make strong parametric assumptions about how the associations of interest vary. Unfortunately such functional form assumptions may be inadequate as many of these associations can weaken or level off as people age (see [Dupre, 2007](#), and references therein).

In [Section 5.1](#), we use VCBART to estimate whether and how the associations between total score on a battery of cognitive assessments and measures of SEP in childhood, early adulthood, and later-life can vary with respect to sociodemographic factors like age, race, and gender. Our dataset comes from the Health and Retirement Study (HRS), which is a nationally representative longitudinal study of US-based adults, and contains $N = 67,988$ total observations of $n = 10,812$ subjects. After adjusting for SEP in early and late adulthood, we found little association between childhood SEP and later-life cognition. Further, after adjusting for SEP in childhood and late adulthood, the

association between early adulthood SEP and later-life cognition varied with respect to race and gender but did not vary substantially over time.

Crime in Philadelphia. Over multiple studies of neighborhood-level crime, Balocchi and colleagues have discovered that (i) partially pooling data across adjacent neighborhoods often improves crime forecasts but (ii) ignoring potential spatial discontinuities can yield highly biased forecasts (Balocchi and Jensen, 2019; Balocchi et al., 2021, 2023). Spatial discontinuities not only occur along known geographic landmarks (e.g. highways, parks, or rivers) but can also coincide with less visible differences in neighborhood-level demographic and socioeconomic dimensions. Balocchi et al. (2023) fit linear models regressing a transformed crime density onto a time index in each of Philadelphia’s 384 census tracts. Concerned about potential spatial discontinuities in the tract-specific slopes and intercepts, they estimated two partitions of the tracts, one for the slopes and one for the intercepts, in which parameter values were similar within clusters but not across clusters. Working within a Bayesian framework, they identified several high posterior probability partition pairs with an ensemble optimization procedure that greedily searched over the space of pairs of partitions of census tracts.

Although they obtained promising predictive results, their analysis is limited by the assumption that the number of reported crimes within each census tract is monotonic in time. An arguably more realistic model would (i) incorporate higher-order trends to better capture potential non-linearities and (ii) allow the corresponding model coefficients to vary across tracts. That is, a more realistic model would allow for different non-monotonic crime trends in different parts of the city. Unfortunately, extending Balocchi et al. (2023)’s optimization procedure to cover higher-order models is computationally impractical, as it must search over a combinatorially vast product space of partitions. In Section 5.2, we recast their model as a linear varying coefficient model with a single categorical effect modifier Z recording the census tract. Using VCBART to fit several tract-specific polynomial models, we find that a quadratic model of crime provides a better fit to data than their linear model and other higher-order extensions.

1.2 Our contributions

In both problems, we wish to make minimal assumptions about the functional form of the covariate effects $\beta_j(\mathbf{Z})$. Additionally, at least for the HRS data, we wish to identify which elements of Z modify the effects of which elements of X . Further, in both applications, calibrated and coherent uncertainty quantification is imperative. For the HRS data, identifying disparities in the socioeconomic determinants of later-life cognition carry profound public health implications, especially in light of an aging population. And for the crime dataset, accurate assessments of the uncertainty about crime forecasts can inform future public safety policy decisions. Finally, we require a method that can scale to the size of the two motivating datasets, ideally without involving computationally

intensive hyperparameter tuning.

Unfortunately, no existing procedure for fitting varying coefficient models meets our desiderata of flexibility, uncertainty quantification, and scalability. To wit, existing state-of-the-art procedures with multivariate modifiers either learn many tuning parameters with leave-one-out cross-validation or rigidly assume that the $\beta_j(\mathbf{Z})$ are additive in the Z_r 's. Moreover, the default implementations of existing procedures do not provide any out-of-sample uncertainty quantification.

We instead approximate each $\beta_j(\mathbf{Z})$ with a sum of regression trees. On synthetic data, our proposed procedure VCBART exhibits superior covariate effect recovery compared to the current state-of-the-art *without requiring any hand-tuning or strong structural assumptions*. We additionally show that, under mild conditions, the VCBART posterior concentrates at a near-optimal rate, even with correlated residual errors. To the best of our knowledge, our Theorem 1 is the first result demonstrating the theoretical near-optimality of Bayesian treed regression in settings with non-i.i.d. noise.

Here is an outline for the rest of the paper. We briefly review relevant background on VC modeling and BART in Section 2. Then, in Section 3, we introduce VCBART, describe how to perform posterior inference, and state our asymptotic results. In Section 4, we demonstrate VCBART's excellent covariate effect recovery and predictive capabilities using synthetic data. We apply VCBART to our motivating datasets in Section 5 before outlining several avenues for future work in Section 6.

2 Background

2.1 Varying coefficient models

Since their introduction in [Hastie and Tibshirani \(1993\)](#), varying coefficient models have been extensively studied and deployed in statistics and econometrics. We give a very brief overview here; see [Fan and Zhang \(2008\)](#) and [Franco-Villoria et al. \(2019\)](#) for more comprehensive reviews.

When there is only a single modifier (i.e. $R = 1$), one popular approach to fitting the model in Equation (1) is to express each $\beta_j(\mathbf{Z})$ as a linear combination of pre-specified basis functions (see, e.g. [Hoover et al., 1998](#); [Huang et al., 2002](#)). Such a decomposition effectively reduces the functional regression problem to a high-dimensional linear regression problem for which numerous frequentist (see, e.g., [Wang et al., 2008](#); [Wang and Xia, 2009](#); [Wei et al., 2011](#)) and Bayesian ([Bai et al., 2019](#)) regularization techniques have been proposed. Kernel smoothing is another popular and theoretically supported alternative when $R = 1$ ([Wu and Chiang, 2000](#)).

Varying coefficient models are commonly encountered in spatial statistics (see, e.g., [Gelfand et al., 2003](#); [Finley and Banerjee, 2020](#)). In these settings, there are usually $R = 2$ modifiers (space) or $R = 3$ modifiers (space and time) and the $\beta_j(\mathbf{Z})$'s are typically modeled with Gaussian pro-

cesses. When the number of observations is large, full Bayesian inference with these models can be computationally demanding, necessitating the use of clever approximations or advanced techniques like distributed computing (Guhaniyogi et al., 2022). Outside of spatial contexts, to accommodate $R > 1$ modifiers, Tibshirani and Friedman (2020) and Lee et al. (2018) respectively constrained the $\beta_j(\mathbf{Z})$ ’s to be linear and additive functions of the Z_r ’s. In contrast, Li and Racine (2010) proposed a multivariate kernel smoothing estimator that imposes no rigid structural assumptions on the covariate effects. However, the default implementation of their procedure tunes several bandwidth parameters with leave-one-out cross-validation. When n, p , or R are large, their procedure is computationally prohibitive.

In the last decade, several authors have used regression trees to estimate the covariate effects. Bürgin and Ritschard (2015), for instance, modeled each $\beta_j(\mathbf{Z})$ with a single regression tree while Wang and Hastie (2012) and Zhou and Hooker (2022) both constructed separate ensembles for each $\beta_j(\mathbf{Z})$ using boosting. Unfortunately, existing tree-based procedures require substantial tuning and often do not automatically return any uncertainty estimates.

2.2 Bayesian Additive Regression Trees

Chipman et al. (2010) introduced BART in the context of the standard nonparametric regression problem: given n observations from the model $y \sim \mathcal{N}(f(\mathbf{x}), \sigma^2)$, they estimated f with a sum of M piecewise constant step functions, which they represented as binary regression trees. Formally, they computed a posterior distribution over regression tree ensembles, which induces an approximate posterior distribution over regression function evaluations $f(\mathbf{x})$. Their regression tree prior, which we adopt and detail in Section 3.1, introduces strong regularization and encourages trees to be “weak learners” in the sense that no one tree explains too much variation in the observed y ’s.

The basic BART model has been extended successfully to survival analysis (Sparapani et al., 2016), multiple imputation (Xu et al., 2016), log-linear models (Murray, 2021), semi-continuous responses (Linero et al., 2020), and causal inference (Hill, 2011; Hahn et al., 2020). With conceptually simple modifications, BART can also recover smooth (Linero and Yang, 2018; Starling et al., 2020) and monotonic (Starling et al., 2019; Chipman et al., 2022) functions. In each setting, BART-based methods often substantially outperform existing procedures in terms of function recovery, prediction, and ease-of-use. Indeed, nearly every BART extension provides default hyperparameters that yield generally excellent performance “off-the-shelf.” Further, recent results in Ročková and Saha (2019) and Ročková and van der Pas (2020) demonstrate BART’s theoretical near-optimality under very mild assumptions. See Tan and Roy (2019) and Hill et al. (2020) for more detailed reviews of BART and its many extensions.

3 The VCBART procedure

Without loss of generality, suppose that we have R_{cont} continuous modifiers, each of which has been re-scaled to lie in the unit interval $[0, 1]$, and R_{cat} categorical or discrete modifiers. For $r = 1, \dots, R_{\text{cat}}$, we will assume that the r -th categorical modifier can take K_r distinct values contained in some discrete set $[K_r]$. We further concatenate our modifiers into a vector \mathbf{Z} whose first R_{cont} entries record the values of the continuous modifiers and whose last R_{cat} entries record the values of the categorical modifiers. In other words, each observed modifier vector \mathbf{z} lies in the product space $\mathcal{Z} = [0, 1]^{R_{\text{cont}}} \times [K_1] \times \dots \times [K_{R_{\text{cat}}}]$.

Both motivating applications involve repeated measurements over time: in the HRS dataset, we have between four and eight observations per subject and in the crime dataset, we have yearly crime densities in each census tract. For simplicity, we will refer to the observed units (i.e. HRS participants and Philadelphia census tracts) as “subjects.” For each subject $i = 1, \dots, n$, we observe n_i triplets $(\mathbf{x}_{it}, \mathbf{z}_{it}, y_{it})$ of covariates \mathbf{x} , modifiers \mathbf{z} , and outcome y . For all $i = 1, \dots, n$, and $t = 1, \dots, n_i$, we model

$$y_{it} = \beta_0(\mathbf{z}_{it}) + \sum_{j=1}^p \beta_j(\mathbf{z}_{it})x_{itj} + \sigma\varepsilon_{it}. \quad (2)$$

We further assume $\boldsymbol{\varepsilon}_i = (\varepsilon_{i1}, \dots, \varepsilon_{in_i})^\top \sim \mathcal{N}_{n_i}(\mathbf{0}_{n_i}, \boldsymbol{\Sigma}_i(\rho))$ where $\boldsymbol{\Sigma}_i(\rho)$ is a correlation matrix with off-diagonal elements equal to $0 \leq \rho < 1$. In other words, we assume an exchangeable or compound symmetry correlation structure for each subject’s errors. We assume that the noise vectors $\boldsymbol{\varepsilon}_i$ ’s are independent across subjects. We do not assume that we observe each subject an equal number of times nor do we assume that the observation times are equally spaced.

The key idea of VCBART is to approximate each function $\beta_j(\mathbf{Z})$ with its own regression tree ensemble. In Section 3.1 we describe the prior over the regression trees and in Section 3.2, we outline strategies for posterior computation and modifier selection.

3.1 Regression tree prior

To set our notation, let T be a binary decision tree that consists of a collection of internal nodes and a collection of terminal or *leaf nodes*. Each internal node of T is associated with a decision rule $\{Z_r \in \mathcal{C}\}$. When Z_r is a continuous variable, \mathcal{C} is a half-open interval of the form $[0, c)$ and when Z_r is categorical, \mathcal{C} is a subset of $[K_r - R_{\text{cont}}]$.

Given T and any vector \mathbf{z} , we can imagine tracing a path from the root down the tree by following the decision rules. Specifically, any time the path encounters the rule $\{Z_r \in \mathcal{C}\}$, it proceeds to the left child if $z_r \in \mathcal{C}$. Otherwise, it proceeds to the right child. Such decision-following paths continue until they reach a leaf node. It is not difficult to verify that every such path terminates in

a single leaf node, implying that T induces a partition of \mathcal{Z} into disjoint regions, one for each leaf. By associating each leaf node ℓ of T with a scalar *jump* μ_ℓ , the pair $(T, \boldsymbol{\mu})$ represents a piecewise constant function over \mathcal{Z} , where $\boldsymbol{\mu}$ denotes the collections of jumps (see Figure 1 for an example).

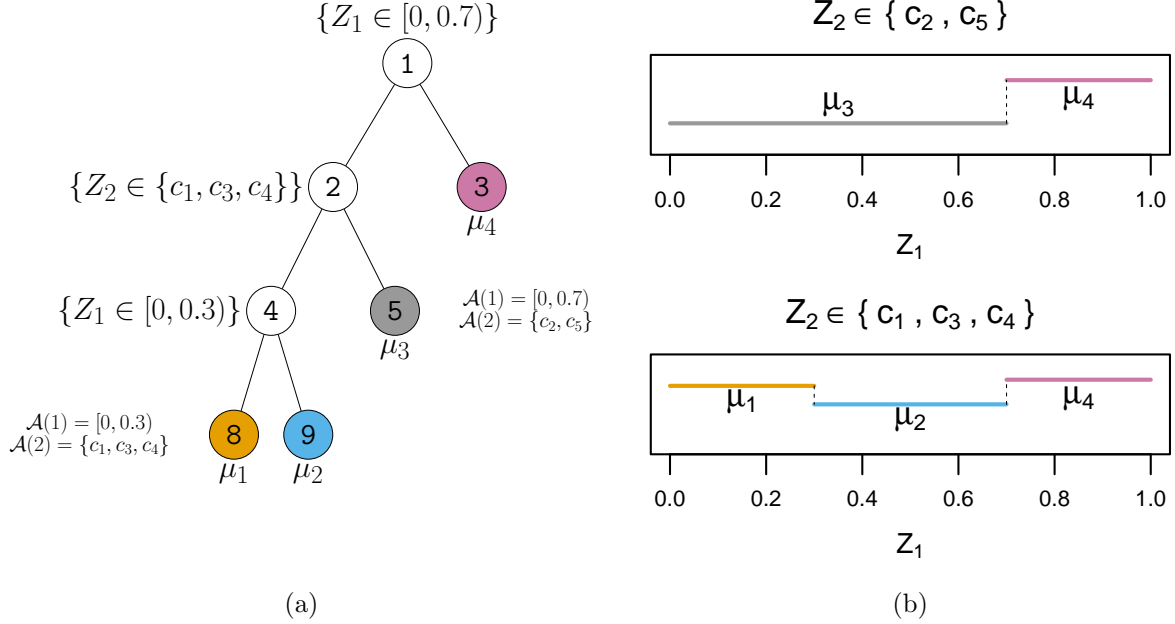


Figure 1: A regression tree defined over $\mathcal{Z} = [0, 1] \times \{c_1, \dots, c_5\}$ (a) and its step function representation (b). In (a), we also report the sets of available values of Z_1 and Z_2 at nodes 5 and 8.

For each $j = 0, \dots, p$, we introduce an ensemble $\mathcal{E}_j = \{(T_m^{(j)}, \boldsymbol{\mu}_m^{(j)})\}_{m=1}^M$ of M regression trees to approximate the function $\beta_j(\mathbf{Z})$. We model each ensemble independently and place independent and identical priors on the individual regression trees within each ensemble. We complete our prior specification with a uniform prior on the autocorrelation ρ and a half- t_7 prior on σ .

We specify the prior for an individual tree $(T_m^{(j)}, \boldsymbol{\mu}_m^{(j)})$ in the j -th ensemble compositionally with a marginal prior for the decision tree and a conditional prior for the jumps given the tree. Just like in the original BART model, we model the jumps in $\boldsymbol{\mu}_m^{(j)}$ as *a priori* independent $\mathcal{N}(0, \tau_j^2)$ random variables, where τ_j is a positive hyperparameter. Thus, for each $\mathbf{z} \in \mathcal{Z}$, the implied marginal prior of $\beta_j(\mathbf{z})$ is $\mathcal{N}(0, M\tau_j^2)$. We have found taking $\tau_j = 0.5/\sqrt{M}$ to be an effective default choice (see Section S2 of the Supplementary Materials for a hyperparameter sensitivity analysis).

We specify the decision tree prior implicitly by describing how to sample from the prior. First, we draw the overall graphical structure with a branching process that starts from a root node, which is initially considered terminal. Whenever a new terminal node is created at depth d , we attach two child nodes to it with probability $0.95(1 + d)^{-2}$. The quadratic decay ensures that the process terminates at a finite depth.

Given the graphical structure, we draw decision rules at each non-terminal node in two steps. First, we sample the splitting variable index $v \sim \text{Multinomial}(\theta_{j1}, \dots, \theta_{jR})$ and θ_{jr} is the probability of selecting Z_r . We place a symmetric Dirichlet(η_j/R) prior on the vector of splitting probabilities and place a further Beta prior over $\eta_j/(\eta_j + R)$. The implied prior density of η_j is proportional to $(R + \eta_j)^{-(R+1)}$. Although the η_j prior favors sparsity, it has the capacity to include more variables as needed (Linero, 2018, §3.3). As evidenced by the simulation studies in Linero (2018), the prior hierarchy on the splitting variable works well in both the sparse setting, when the function depends on only a few variables, and in the non-sparse setting.

Then, conditional on r , we set \mathcal{C} to be a random subset of $\mathcal{A}(r)$, the set of available Z_r values at the current non-terminal node (see annotations in Figure 1a). When Z_r is continuous, $\mathcal{A}(r)$ is an interval and we set $\mathcal{C} = [0, c)$ where c is drawn uniformly from $\mathcal{A}(r)$. When Z_r is categorical, $\mathcal{A}(v)$ is a discrete set. How we draw the random subset \mathcal{C} depends on whether Z_r displays network structure like the census tracts in our crime data (see Figure 5c). If not, we assign each element of $\mathcal{A}(r)$ to \mathcal{C} with probability 0.5. Otherwise, we form \mathcal{C} by drawing a random network partition. Briefly, we partition the vertices of the subgraph induced by $\mathcal{A}(r)$ by deleting a random edge from a random spanning tree of the subgraph; see Deshpande (2023) for details.

3.2 Posterior computation and modifier selection

Conditional regression tree updates. Because the VCBART posterior is analytically intractable, we simulate posterior draws using a Gibbs sampler. Our sampler is a straightforward extension of Chipman et al. (2010)’s basic Bayesian backfitting strategy that sequentially updates each tree $(T_m^{(j)}, \boldsymbol{\mu}_m^{(j)})$ conditionally on the other $Mp - 1$ regression trees. Specifically, we update $T_m^{(j)}$ with a Metropolis-Hastings step and transition kernel that randomly grows or prunes the tree. Then, given $T_m^{(j)}$, we draw the jumps $\boldsymbol{\mu}_m^{(j)}$ from its conditional posterior distribution. Whereas the jumps in the original BART model are conditionally independent, the correlated errors in Equation (2) render the jumps in VCBART conditionally dependent. After updating all trees in the ensemble \mathcal{E}_j , we perform a conjugate Dirichlet-Multinomial update for the vector of splitting probabilities $\boldsymbol{\theta}_j$. After sweeping over all ensembles, we update σ with a Metropolis-Hastings step and update ρ using Roberts and Rosenthal (2009)’s adaptive Metropolis procedure.

Modifier selection. In our sampler, in order to update the vector of splitting index probabilities $\boldsymbol{\theta}_j$, we keep track of the number of times each modifier Z_r is used in a decision rule in the ensemble \mathcal{E}_j . Using these counts, we can estimate probability that each Z_r is selected at least once in the ensemble \mathcal{E}_j used to estimate $\beta_j(\mathbf{Z})$. These selection probabilities are analogous to the posterior inclusion probabilities encountered in Bayesian sparse linear regression. Based on this interpretation, for each ensemble \mathcal{E}_j , we construct an analog of Barbieri and Berger (2004)’s median probability model by reporting those modifiers Z_r whose selection probability exceeds 0.5.

Before proceeding, we pause to make two remarks about parameter identifiability and our use of *a priori* independent tree ensembles.

Remark 1 (Identifiability). *For each realization of the modifiers \mathbf{z} , the vector of covariate function evaluations $\beta(\mathbf{z}) = (\beta_0(\mathbf{z}), \dots, \beta_p(\mathbf{z}))$ is identifiable as long as $\mathbb{E}[\mathbf{x}\mathbf{x}^\top | \mathbf{Z} = \mathbf{z}]$ is positive definite (Huang and Shen, 2004). The individual regression trees, however, are not identified. This is because we can switch the order of the trees without changing the predictions. Nevertheless, in our simulation studies, we did not experience any difficulties recovering the true covariate effects.*

Remark 2 (Prior dependence between the β_j 's). *We introduce $p+1$ *a priori* independent univariate regression tree ensembles, one for each covariate effect function $\beta_j(\mathbf{Z})$. Despite the prior independence, the observed data likelihood introduces posterior dependence between evaluations $\beta_j(\mathbf{z})$. Nevertheless, it is natural to wonder how one might introduce prior dependence between the $\beta_j(\mathbf{Z})$'s. There are at least two ways. First, one could model the vector-valued $\beta(\mathbf{Z}) = (\beta_0(\mathbf{Z}), \dots, \beta_p(\mathbf{Z}))^\top$ with a single ensemble of regression trees with multivariate jumps. Alternatively, one may express each $\beta_j(\mathbf{Z})$ as a linear combination of a common set of basis functions, each of which is modeled as a sum of regression trees. Linero et al. (2020)'s shared forest model uses such an expansion to learn multiple functions simultaneously. In situations where one expects that a modifier Z_r may be relevant to some but not all covariate effects, we argue that our separate ensemble approach is preferable. Modeling $\beta(\mathbf{Z})$ with a single ensemble of multivariate regression trees or a shared forest essentially assumes that all $\beta_j(\mathbf{Z})$'s vary with respect to the same Z_r 's in exactly the same way.*

3.3 Posterior contraction of VCBART

With some minor modifications, VCBART enjoys essentially the same favorable theoretical properties as BART — namely, the posterior concentrates at a nearly minimax optimal rate. To facilitate our theoretical analysis of the VCBART posterior, we assume that all modifiers are continuous and have been re-scaled to lie in $[0, 1]^R$. Like Ročková and Saha (2019), we modify the decision tree prior so that the probability that the branching process continues growing at depth d is γ^d for some fixed $N^{-1} < \gamma < 1/2$. We further assume that there are truly functions $\beta_{0,0}(\mathbf{Z}), \dots, \beta_{0,p}(\mathbf{Z})$ satisfying for each $i = 1, \dots, n$ and $t = 1, \dots, n_i$,

$$y_{it} = \beta_{0,0}(\mathbf{z}_{it}) + \sum_{j=0}^p \beta_{0,j}(\mathbf{z}_{it}) x_{itj} + \sigma_0 \varepsilon_{it}, \quad (3)$$

where each function $\beta_{0,j}(\mathbf{Z})$ is α_j -Hölder continuous with $0 < \alpha_j \leq 1$, and $\varepsilon_i \sim \mathcal{N}(\mathbf{0}_{n_i}, \mathbf{\Sigma}_i(\rho_0))$. With the additional assumptions (i) that the eigenvalues of $\mathbf{\Sigma}_i(\rho_0)$ are bounded away from zero and infinity and (ii) about the rates at which p and R diverge as n increases, the VCBART posterior concentrates around the true function values at a near-optimal rate as the total number of observations increases. While we defer precise statements of the technical assumptions to Section

S1 of the Supplementary Materials, we note here that the assumptions are not restrictive. For instance, we can always re-scale continuous modifiers to the unit interval and, with one-hot encoding, represent categorical modifiers with multiple binary indicators. Further, many commonly used error structures satisfy the required assumptions on the Σ_i 's including first-order autoregressive, compound symmetry, and moving averages.

Let $N = \sum_{i=1}^n n_i$ be the total number of observations across all n subjects, and let β and β_0 be $N \times (p+1)$ matrices whose respective (i, j) -th entries are $\beta_j(\mathbf{z}_{it})$ and $\beta_{0,j}(\mathbf{z}_{it})$. Let $\|\beta - \beta_0\|_N^2 = N^{-1} \sum_{i=1}^n \sum_{t=1}^{n_i} \sum_{j=0}^p [\beta_j(\mathbf{z}_{it}) - \beta_{0,j}(\mathbf{z}_{it})]^2$ be the squared empirical ℓ_2 norm. If we knew the true smoothness levels α_j , the minimax rate for estimating β_0 in $\|\cdot\|_N^2$ norm is $r_N^2 = \sum_{j=0}^p N^{-2\alpha_j/(2\alpha_j+R)}$ (Ročková and van der Pas, 2020). In the absence of this knowledge, Theorem 1 shows that VCBART can estimate the varying coefficients β_0 at nearly this rate, sacrificing only a logarithmic factor.

Theorem 1. *Under (3), suppose we endow (β, σ) with a modified VCBART prior, where the splitting probability of each node at depth d in a decision tree is given by γ^d , for some $N^{-1} \leq \gamma < 0.5$ and the splitting indices are chosen uniformly (i.e. $\theta = (1/R, \dots, 1/R)$), and $\nu > 1$ in the half- t_ν prior on σ . Suppose we further endow ρ with the uniform prior, $\rho \sim \mathcal{U}(0, 1)$. Assume that assumptions (A1)–(A4) in Section S1 of the Supplementary Materials hold. Then for some constant $M > 0$ and $r_N^2 = \log N \times \sum_{j=0}^p N^{-2\alpha_j/(2\alpha_j+R)}$,*

$$\Pi(\beta : \|\beta - \beta_0\|_N > Mr_N | \mathbf{Y}) \rightarrow 0, \quad (4)$$

in $\mathbb{P}_{\beta_0}^{(N)}$ -probability as $N, p \rightarrow \infty$.

We present the proof of Theorem 1 in Section S1 of the Supplementary Materials.

4 Simulation studies

We performed two simulation studies to understand VCBART's ability to (i) estimate covariate effect functions and predict future outcomes; (ii) identify which elements of \mathbf{Z} modify the effects of which elements of X ; and (iii) scale to large datasets. We generated data for these experiments from the model in Equation (2) with $p = 5$ correlated covariates, $R = 20$ potential effect modifiers, $\sigma = 1$, and independent within-subject errors. The correlated covariates were drawn from a multivariate normal distribution with mean zero and a covariance matrix with entries $0.5^{|i-j|}$. The modifiers were drawn uniformly from the interval $[0, 1]$. We used the following covariate effect functions in

all experiments

$$\begin{aligned}
\beta_0(\mathbf{z}) &= 3z_1 + (2 - 5\mathbb{1}(z_2 > 0.5))\sin(\pi z_1) - 2\mathbb{1}(z_2 > 0.5) \\
\beta_1(\mathbf{z}) &= \frac{\sin(2z_1 + 0.5)}{4z_1 + 1} + (2z_1 - 0.5)^4 \\
\beta_2(\mathbf{z}) &= (3 - 3z_1^2 \cos(6\pi z_1)) \times \mathbb{1}(z_1 > 0.6) - 10\sqrt{z_1} \times \mathbb{1}(z_1 < 0.25) \\
\beta_3(\mathbf{z}) &= 1 \\
\beta_4(\mathbf{z}) &= 10\sin(\pi z_1 z_2) + 20(z_3 - 0.5)^2 + 10z_4 + 5z_5 \\
\beta_5(\mathbf{z}) &= \exp\left\{\sin\left((0.9(z_1 + 0.48))^{10}\right)\right\} + z_2 z_3 + z_4.
\end{aligned}$$

The top row of Figure 2 shows the functions β_0, \dots, β_3 . The bottom row of Figure 2 superimposes the VCBART posterior mean and 95% credible intervals for β_0, \dots, β_3 computed using a single dataset from our first experiment, which comprised four observations of $n = 250$ subjects for a total of $N = 1,000$ observed $(\mathbf{x}_{it}, \mathbf{z}_{it}, y_{it})$'s. The posterior mean and uncertainty bands were computed after running four independent chains of VCBART for 2,000 iterations, discarding the first 1,000 samples of each as burn-in. We approximated each $\beta_j(\mathbf{Z})$ with an ensemble of $M = 50$ trees and set each $\tau_j = 0.5/\sqrt{M}$.

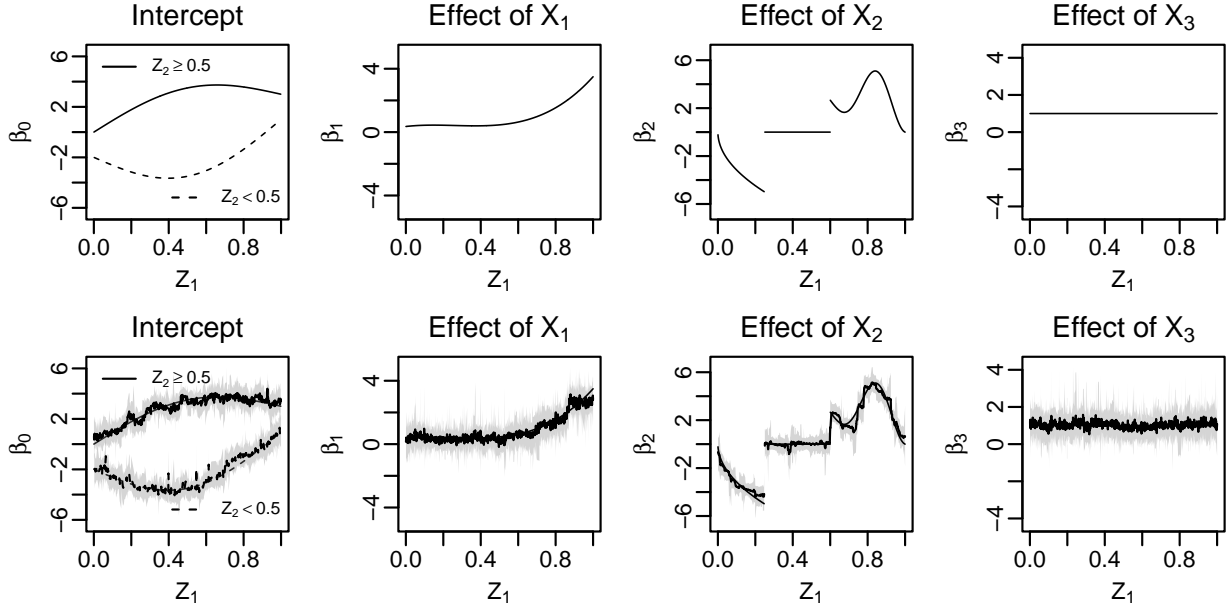


Figure 2: **Top row.** True functions β_0, \dots, β_3 . **Bottom row.** VCBART's posterior mean (dark line) and pointwise 95% credible interval (shaded) for each function

Although the covariate effect functions have very different shapes, VCBART recovered each remarkably well: the posterior means of each $\beta_j(\mathbf{Z})$ closely tracked the shape of the true functions

and, for the most part, the true function values were within the shaded pointwise 95% credible intervals. We observed similar behavior for the functions $\beta_4(\mathbf{Z})$ and $\beta_5(\mathbf{Z})$ that depend on multiple effect modifiers (see Figure S1 in the Supplementary Materials). Repeating this experiment twenty five times — that is, fixing the \mathbf{x}_{it} ’s and \mathbf{z}_{it} ’s but simulating the y_{it} ’s anew — the mean coverage of the 95% posterior credible intervals, averaged across all the β_j ’s, exceeded 99%. Further, averaging across all functions and replications, the mean sensitivity, specificity, precision and F1-score¹ for modifier selection with our median probability model were 0.85, 0.99, 0.95, and 0.90, indicating excellent support recovery performance. Sequentially running 4 MCMC chains for 2,000 iterations each took just under one minute on an M1 Mac.

We compared VCBART’s ability to estimate covariate effects out-of-sample to those of the following methods: the standard linear model (`lm`); Li and Racine (2010)’s kernel smoothing (KS; implemented in Hayfield and Racine (2008)’s `np` package); Bürgin and Ritschard (2015)’s tree ensemble procedure (TVCM; implemented in Bürgin and Ritschard (2017)’s `vcpart` package); and Zhou and Hooker (2022)’s boosted tree procedure method (BTVCM; R code available at <https://github.com/siriuz42/treeboostVCM>). By default, TVCM and KS respectively perform cross-validation to prune the regression trees and to learn kernel bandwidth parameters. The default implementation of BTVCM, on the other hand, does not tune the number of trees or learning rate; in our experiments, we ran the method with 200 trees and with the learning rate used in Zhou and Hooker (2022)’s experiments.

We generated 25 different datasets comprising 250 training subjects and 25 testing subjects, each contributing four observations. That is, we repeatedly trained each method using 1,000 total simulated observations and evaluated performance using an additional 100 observations. As with Figure 2, we ran four chains VCBART for 2,000 iterations, discarding the first 1,000 as “burn-in,” with $M = 50$ trees per ensemble and setting each $\tau_j = 0.5/\sqrt{M}$. Since the off-the-shelf implementations of KS, TVCM, and BTVCM do not return standard errors of the estimated covariate effects, we formed 95% bootstrap confidence intervals for each $\beta_j(\mathbf{z})$ using 50 bootstrap resamples. We ran these experiments in a shared high-throughput computing cluster (Center for High Throughput Computing, 2006). Figures 3a and 3b compare the out-of-sample mean square error for estimating $\beta_j(\mathbf{z})$ and uncertainty interval coverages, averaged across all six functions and over all 100 testing set observations. We report function-by-function performance in Section S3.2 of the Supplementary Materials.

In terms of estimating out-of-sample evaluations $\beta_j(\mathbf{z})$, `lm`, which assumes that each covariate effect is constant with respect to \mathbf{Z} , performed the worst while VCBART appeared the best. VCBART additionally produced much more accurate predictions and better-calibrated uncertainty intervals

¹Letting TP, TN, FP, and FN be the numbers of true positive, true negative, false positive, and false negative identifications in the supports of the β_j ’s, sensitivity is $TP/(TP + FN)$, specificity is $TN/(TN + FP)$, precision is $TP/(TP + FP)$ and the F1 score is $2 \times TP/(2 \times TP + FP + FN)$

than TVCM and BTVM, the other tree-based varying coefficient procedures. On closer inspection, we further found that the higher coverage of VCBART’s uncertainty intervals was not a by-product of exceedingly wide intervals. In fact, VCBART’s credible intervals for evaluations $\beta_j(\mathbf{z})$ tended to be shorter than the bootstrapped confidence intervals produced by KS, BTVM, and TVCM.

Sequentially running four VCBART chains took, on average, about three minutes on our shared cluster. Both `lm` and BTVM were faster for these data, with `lm` running nearly instantaneously and BTVM producing point estimates $\hat{\beta}_j(\mathbf{z})$ in about 90 seconds. That said, both `lm` and BTVM produced substantially worse point estimates than VCBART. Although a carefully tuned BTVM could yield better performance, we expect such tuning would take much longer. We additionally found that obtaining point estimate $\hat{\beta}_j(\mathbf{z})$ with TVCM and KS took 1.6 and 9.6 hours, respectively, on average. Sequentially running four chains of VCBART was substantially faster and produced better-calibrated uncertainty intervals than performing 50 bootstrap resamples for BTVM, TVCM, and KS. In summary, compared to existing methods for fitting varying coefficient models, VCBART was faster and produced more accurate predictions and better-calibrated uncertainty intervals off-the-shelf.

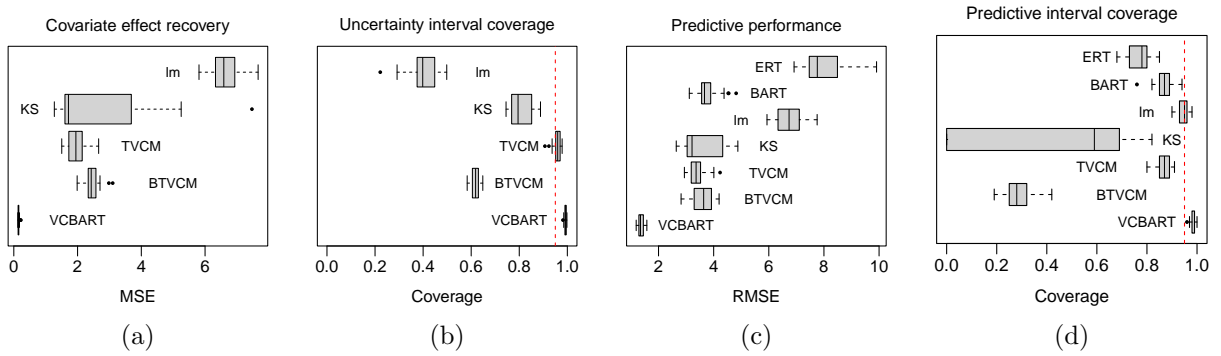


Figure 3: (a) Average mean square error for estimating evaluations $\beta_j(\mathbf{z})$. (b) Average coverage of 95% uncertainty intervals for evaluations $\beta_j(\mathbf{z})$. (c) Predictive root mean square error. (d) Coverage of 95% prediction intervals. All measures reported over 25 testing datasets.

Intuitively, we should expect any method that reliably recovers individual out-of-sample evaluations $\beta_j(\mathbf{z})$ to yield highly accurate predictions of the outcome Y . And indeed, Figure 3c shows that the out-of-sample predictive root mean square error (RMSE) of VCBART and the aforementioned competitors generally track with their estimation error. Figure 3c additionally shows that VCBART achieved smaller predictive RMSE than two fully non-parametric methods, BART (implemented in McCulloch et al. (2018)’s **BART** package) and extremely randomized trees (ERT; implemented in Wright and Ziegler (2017)’s **ranger** package). In our experiments, we allowed BART and ERT to use both X and Z to predict Y . Although BART and ERT are facially more flexible than the other competitors, their predictive performance was worse than the correctly-specified varying coefficient methods. Interestingly, however, BART and ERT produced predictive intervals with better coverage than the well-specified BTVM and KS (Figure 3d). That said, VCBART tended to return predictive

intervals with better coverage than both **BART** and **ERT**.

To better understand how well VCBART scales to larger datasets, we conducted a second simulation study. Similar to our first study, we generated 25 synthetic datasets with n training subjects and 250 testing subjects, each contributing four observations. We varied n between 25 and 12,500, allowing us to see how VCBART performed when trained on as few as 100 and as many as 50,000 total observations. For brevity, we summarize the main findings of that study here and defer more detailed results to Section S3.3 of the Supplementary Materials. Unsurprisingly, as N increased, VCBART’s estimation and prediction error decreased and the frequentist coverage of its credible intervals and posterior predictive intervals remained high. In fact, VCBART produced uncertainty intervals with higher-than-nominal frequentist coverage even when fit to as few as $N = 100$ total observations. We additionally found that the median probability model’s operating characteristics generally improved as N increased. For instance, the F1 score was 0.68 when $N = 200$ and exceeded 0.85 for $N > 1000$.

As each regression tree update involves computing and updating residuals $y_{it} - \beta_0(\mathbf{z}_{it}) - \sum_j x_{ijt}\beta_j(\mathbf{z}_{it})$ (i.e. a total of $O(N)$ operations per iteration), we would expect VCBART to scale linearly in the total number of observations, keeping the total number of MCMC iterations fixed. In our experiments, we observed a strong linear relationship ($R^2 = 0.997$) between total run time and total number of observations: on an M1 Mac, sequentially running four VCBART chains for 2,000 iterations each took around 55 seconds for $N = 1,000$ observations, 8.5 minutes for $N = 10,000$ observations, and around 48 minutes with $N = 50,000$ observations.

5 Real data examples

5.1 HRS cognition data

To investigate how associations between later-life cognition and socioeconomic position at multiple life stages may vary over time and across sociodemographic characteristics, we analyzed publicly available data from the Health and Retirement Study (HRS). The HRS is a nationally representative longitudinal survey of US adults over the age of 50 and their spouses of any age. Since 1992, the HRS has biennially assessed the economic, health, and social implications of aging through its core survey with response rates greater than 85% in each wave. The HRS is sponsored by the National Institute on Aging (NIA; U01AG009740) and is conducted by the University of Michigan. See [Sonnegga et al. \(2014\)](#) for additional details about the HRS.

In each wave, the HRS consistently administered a battery of cognitive tests that include tasks like listening to a series of 10 words and recalling as many possible immediately and several minutes later. The HRS constructed a summary score that ranges from 0 to 35, with higher scores reflecting better cognitive functioning. In our analysis, we use the total cognitive score as our outcome. Our

covariate set includes measures of SEP at three distinct stages of life. The first is a composite childhood SEP index, developed and validated by Vable et al. (2017), which is based on the educational attainment and occupation of each subject’s parents and their overall financial well-being in childhood. Higher scores on this index correspond to higher SEP. We additionally included indicators of high school and college completion as proxies of SEP in early adulthood. Finally, as measures of SEP in older adulthood, we used log-income and an indicator of labor force participation. Our modifiers included age in months, gender, race, the U.S. Census division of subject’s birthplace, and an indicator of whether the subject identified as Hispanic.

We restricted our analysis to HRS subjects who (i) had complete covariate, modifier, and outcome data in at least four HRS waves and (ii) were dementia-free in the first wave with complete data. This resulted in analytic sample of $n = 10,812$ subjects who contributed a total of $N = 67,988$ person-years over the study period. In total, we had $p = 5$ covariates and $R = 5$ potential modifiers. Using the same hyperparameter setting as in Section 4 (i.e. $M = 50, \tau_j = 0.5/\sqrt{M}$), we simulated 50 Markov chains of 1,050 iterations. Discarding the first 1,000 samples from each chain as “burn-in,” we obtained a total of 2,500 MCMC samples from the VCBART posterior.

Based on these samples, for each combination of r and j , we computed the posterior probability that the modifier Z_r was used in at least one decision rule in the ensemble \mathcal{E}_j . We then computed the median probability model for each $\beta_j(\mathbf{z})$ by thresholding these probabilities at 0.5, as described in Section 3.2. The median probability model included gender for all $\beta_j(\mathbf{Z})$ and selected race for all coefficient functions except for the one associated with later-life labor force participation. It additionally identified birthplace as modifying the effects of childhood SEP and high school completion but not the effects of later-life income or labor force participation. Interestingly, our median probability model identified age as a modifier for each covariate except childhood SEP. That is, after adjusting for SEP at later stages of life, our results suggest that differences in later-life cognitive score driven by differences in childhood SEP do not amplify or attenuate over time. In fact, further inspection revealed that the marginal posterior distributions of the estimated partial effect of childhood SEP for subjects in our dataset concentrated within the interval $[-0.5, 0.5]$ and placed roughly equal probability on both positive and negative values. For reference, the sample standard deviation of cognitive scores was about 4 points on a scale ranging from 0 to 35 points. Our analysis suggests that, after adjusting for SEP in early and older adulthood, childhood SEP has a very small effect, if any, on later-life cognitive scores.

Figure 4 shows the posterior mean and point-wise 95% credible intervals of the predicted intercept and partial effects of childhood SEP and high school completion for two baseline individuals, one Black and one White. Both individuals are females born in the East North Central Census Division of the U.S., which includes the states of Illinois, Indiana, Michigan, Ohio, and Wisconsin. We can interpret the intercept as an average cognitive score for these baseline individuals if they (i) did not

complete high school or college and (ii) did not report any earned income or labor force participation in older adulthood.

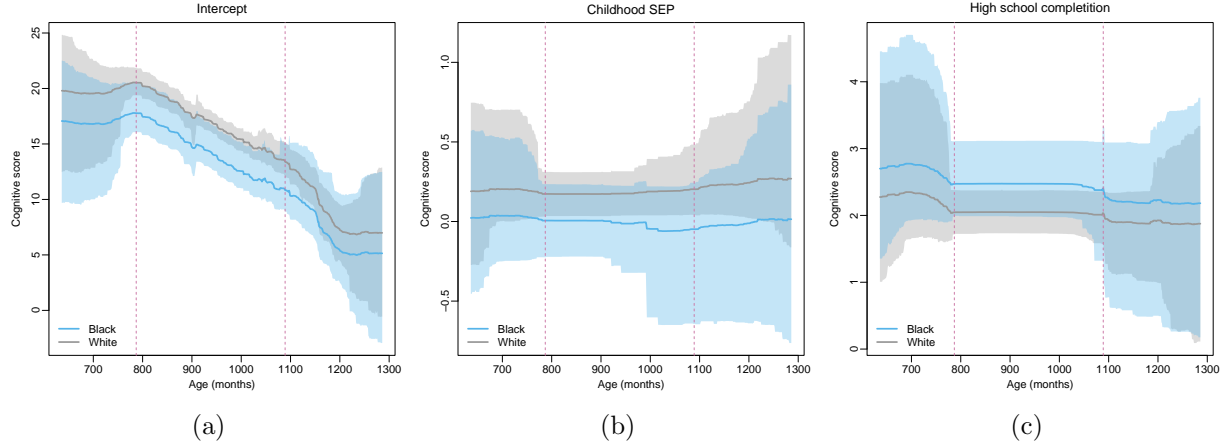


Figure 4: Posterior mean and pointwise 95% credible intervals of the intercept (a) and partial effects of childhood SEP (b) and high school completion (c) on later-life cognitive score as functions of age. Dashed vertical lines delineate the 2.5% and 97.5% quantiles of the observed ages in our dataset.

The dashed vertical lines in each panel show the 2.5% and 97.5% quantiles of the distribution of ages in our dataset. Unsurprisingly, there is much more uncertainty about the estimated effects outside of this age range. In Figure 4a, we observe a steady decline in cognitive scores over time for both baseline individuals as well as a persistent gap between them, with the White individual having slightly higher baseline cognitive scores. As anticipated by our discussion of the median probability model, Figure 4b shows that the posterior distributions of the partial effect of childhood SEP for these individuals is concentrated on small positive and negative effect sizes. In sharp contrast, however, we see in Figure 4c that high school completion is associated with higher cognitive scores for both baseline individuals. Interestingly, we see that the estimated increase in cognitive score associated with high school completion is slightly higher for the Black baseline individual.

Recall that our median probability model detected temporal variation in the partial effect of high school completion. At least for the two baseline individuals considered in Figure 4c, that temporal variation appears to manifest mostly in the lower tail of the distribution. Between the ages of 65 and 90 years old, which covers approximately the middle 95% of observed ages in our dataset, the partial effect appears, for all practical purposes, constant over time.

5.2 Philadelphia crime data

The Philadelphia police department releases the latitude and longitude of every reported crime in the city at opendataphilly.org. In each of the $n = 384$ census tracts in the city (Figure 5a), we computed the yearly crime density, defined as number of crimes per square mile, and applied

an inverse hyperbolic sine transformation to counteract the considerable skewness. Let $y_{v,t}$ be the transformed crime density in census tract v at time t , with $t = 1$ corresponding to 2006 and $t = 16$ corresponding to 2021. Balocchi et al. (2023) modeled $y_{v,t} \sim \mathcal{N}(f^{(v)}(t), \sigma^2)$ and computed first-order approximations of each $f^{(v)}$. That is, they estimated tract-specific parameters $\beta_0^{(v)}$ and $\beta_1^{(v)}$ such that $f^{(v)}(t) \approx \beta_0^{(v)} + \beta_1^{(v)}\tilde{t}$, where \tilde{t} is a centered and re-scaled version of the time index. Rather than separately estimate each tract’s parameters, they assumed that the intercepts and slopes were spatially clustered. To estimate the latent clusterings, they ran several greedy searches across the space of pairs of census tract partitions.

Despite the reasonably accurate predictions obtained with their first-order approximation, a potential drawback of their analysis is the assumed monotonicity of crime over time. An arguably more realistic model would allow for crime potential increases and decreases within each census tract. Although it is conceptually easy to elaborate their model with higher-order terms, fitting such a model is computationally impractical. Specifically, extending their approach to find an order- d polynomial approximation involves searching over the product space of d partitions. The combinatorial vastness of this space renders efficient search all but infeasible.

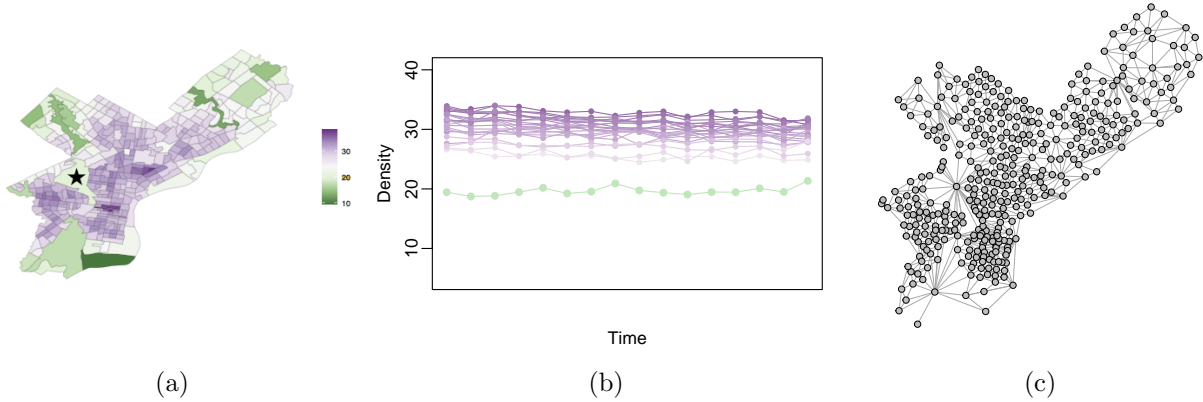


Figure 5: Census tracts of Philadelphia colored according to the averaged transformed crime density (a). Trajectories of crime densities for the starred tract in (a) and its neighbors (b). Census tracts display a network structure based on adjacency (c).

We can instead view their model and higher-order elaborations thereof as varying coefficient models in which the coefficients vary across the vertices of a network determined by census tract adjacency (see Figure 5c). Specifically, for a positive integer d , we can approximate

$$f^{(v)}(t) \approx \beta_0(v) + \beta_1(v)\tilde{t} + \beta_2(v)\tilde{t}^2 + \cdots + \beta_d(v)\tilde{t}^d, \quad (5)$$

where we have suggestively expressed the β_d ’s as functions of the census tract label v .

For a given approximation order d , fitting the model in Equation (5) is relatively straightforward

with VCBART. To encourage spatial smoothness in the $\beta_j(v)$'s, we used a version of the BART prior that is supported on regression trees that recursively partition the network encoded by tract adjacencies (Figure 5c) into connected components. Essentially, each individual tree in the ensemble \mathcal{E}_j represents a step function taking different values over clusters of spatially contiguous census tracts. See Deshpande (2023, §3.3) for more details about the prior.

To determine an appropriate order d , we performed a leave-one-out experiment with the Philadelphia crime data. We specifically considered four approximation orders ($d \in \{1, 2, 3, 4\}$) and two different specifications of the within-tract error structure. The first error structure assumes independence across observations while the second assumes that the errors are equally correlated across time points within each tract (i.e. compound symmetry). For each combination of approximation order and error structure, we fit a VCBART model to all data from all but one census tract and predicted the entire held-out trajectory of transformed crime densities. We ran four MCMC chains for 2,000 iterations each, discarding the first 1,000 iterations as “burn-in.” Table 1 reports the training and testing root mean square error, averaged over all tracts, for each combination of approximation order d and error structure.

Table 1: In- and out-of-sample root mean square prediction error and 95% prediction interval coverage for our leave-one-out analysis of the Philadelphia crime data. Best performance in each column is bolded. **ind** stands for independent errors and **cs** stands for compound symmetry errors

	RMSE (train)	RMSE (test)	Coverage (train)	Coverage (test)
$d = 1$, ind	0.61	1.99	0.97	0.78
$d = 2$, ind	0.55	1.97	0.98	0.79
$d = 3$, ind	0.52	1.93	0.98	0.80
$d = 4$, ind	0.50	2.02	0.98	0.81
$d = 1$, cs	0.67	1.95	0.98	0.79
$d = 2$, cs	0.60	1.83	0.98	0.79
$d = 3$, cs	0.57	1.91	0.98	0.79
$d = 4$, cs	0.55	1.93	0.98	0.78

As we might expect, for both error structures, in-sample RMSE decreased with the approximation order d . However, we found that a quadratic approximation fit with compound symmetry errors yielded the best out-of-sample predictive error. Interestingly, for each d , we find that the in-sample RMSE is smaller for the model fit with independent errors while the out-of-sample RMSE is smaller for the model with compound symmetry error structure. These findings suggest that ignoring the repeated observation structure of our data tends to overfit the data, regardless of approximation order. Finally, while the average coverage of the marginal 95% predictive intervals exceeded the nominal level in-sample, the out-of-sample average coverages were much lower than nominal.

Further inspection revealed that the out-of-sample predictive interval coverage exceeded the nominal 95% level in 235 out of 384 (61%) leave-one-out folds. We suspect that the low average coverage

is most likely an artifact of our particular leave-one-out set-up. For the most part, the folds with much lower-than-nominal coverage corresponded to tracts with markedly different crime patterns than their immediate neighbors. As a concrete example, consider the starred tract in Figure 5a. Arguably no method should produce accurate out-of-sample forecasts when this tract is held out; after all, the crime dynamics from the held-out tract are markedly different than the dynamics in the neighboring tracts observed during training. Consequently, when these tracts were held out in our leave-one-out experiment, the prediction intervals were centered around poor point predictions. In other words, the lower-than-nominal coverage was due more to poor forecasts rather than overconfident predictions.

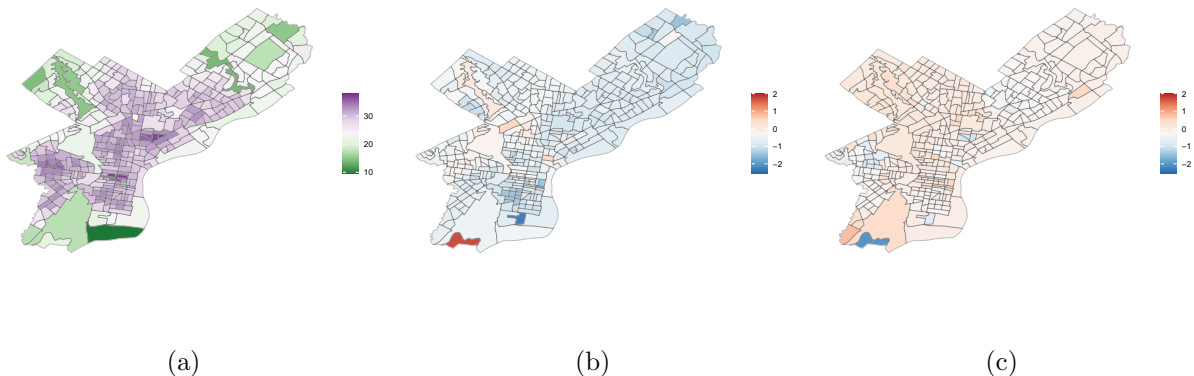


Figure 6: Posterior mean estimates of β_0 (a), β_1 (b), and β_2 (c).

Figure 6 shows the posterior means of the coefficients from the best-fitting model. With some exceptions, we estimated that β_1 was negative and β_2 was positive in most census tracts. These findings are consistent with the general observations that crime fell city-wide in the early half of the 2010's before increasing towards the end of the decade and into early-2020. Further, the marginal posterior distributions of the linear coefficient β_1 and quadratic coefficient β_2 tended to concentrate on small values close to zero. In light of the relatively flat trace plots in Figure 5b and for the other census tracts (not shown), such a finding is not entirely unexpected. That said, we found that in around 88% of all census tracts (338 out of 384), the symmetric 95% credible interval for β_1 excluded zero and that in about 32% of all tracts (125 out of 384), the credible intervals for both β_1 and β_2 excluded zero. In other words, our model identified a small non-linear trend in crime with considerably certainty in about a third of all tracts.

6 Discussion

We have introduced VCBART for fitting linear varying coefficient models that retain the interpretability of linear models while displaying predictive accuracy on par with more flexible, blackbox

regression models. On simulated data, VCBART displayed covariate effect function recovery and predictive performance superior to existing state-of-the-art VC methods *without intensive problem-specific tuning or imposing any structural assumptions about the functions $\beta_j(\mathbf{Z})$* . It moreover returned coherent and generally well-calibrated uncertainty quantifications. Theorem 1 shows that, up to a logarithmic factor, the VCBART posterior concentrates at minimax optimal rate.

In our analysis of the HRS data, we did not explicitly adjust for potential selection biases and confounding. Indeed, it is possible that subjects with higher childhood SEP tended to be better educated and more well-off in later-life. For a more rigorous study of causal effects of SEP on cognitive trajectories, we could use inverse-probability weights as in [Marden et al. \(2017\)](#); indeed, incorporating observation-specific weights to the basic VCBART algorithm is relatively straightforward. Relatedly, the Bayesian causal forest (BCF) models of [Hahn et al. \(2020\)](#) and [Woody et al. \(2020\)](#) are special cases of our more general VCBART model with single covariate. Studying VCBART’s ability to estimate the simultaneous effects of multiple, possibly continuous, treatments under suitable identifying assumptions is an exciting avenue for future development.

In our motivating applications, the number of covariates p was relatively small, compared to the number of total observation N . One can easily imagine, however, settings in which p is comparable to or larger than N . In such settings, running VCBART is challenging as the coefficient functions are no longer identified without further assumptions like sparsity. Under the assumption that only a handful of $\beta_j(\mathbf{Z})$ ’s are truly non-zero functions, we can estimate a sparse varying coefficient model by replacing the normal prior on tree jumps μ_ℓ with spike-and-slab priors. Doing so involves introducing an ensemble-specific indicator and, conditionally on the relevant indicator, modeling all jumps in an ensemble as drawn from, for instance, a mean-zero Gaussian distribution with either a very small or very large variance. Such model elaboration inspires a natural Gibbs sampler that iterates between updating these indicators and updating trees within each ensemble. Unfortunately, we would expect this Gibbs sampler to inherit the slow mixing of Gibbs samplers for spike-and-slab regression and for treed regression ([Ronen et al., 2022](#); [Kim and Ročková, 2023](#)). A potentially more promising computational solution would combine existing fast mode-finding algorithms like EMVS ([Ročková and George, 2014](#)) for sparse regression and the accelerated BART and BCF algorithms ([He et al., 2019](#); [Krantsevich et al., 2021](#)) for treed regression. Extending these accelerated algorithms to the general varying coefficient model setting is the subject of on-going work.

Finally, throughout this work we have assumed that the sets of covariates X and effect modifiers Z was fixed and known. While domain knowledge and theory often suggest natural choices of effect modifiers, we can readily envision scenarios in which it is not immediately clear whether a particular predictor should enter Equation (1) as a covariate, modifier, or both. In these situations, we recommend setting both X and Z equal to the full set of available predictors.

Acknowledgements

Support for this work was provided by the University of Wisconsin–Madison Office of the Vice Chancellor for Research and Graduate Education with funding from the Wisconsin Alumni Research Foundation (S.K.D.); and National Science Foundation grant DMS-2015528 (R.B.).

References

- Aartsen, M. J., Cheval, B., Sieber, S., Van der Linden, B. W., Gabriel, R., Courvoisier, D. S., Guessous, I., Burton-Jeangros, C., Blane, D., Ihle, A., Kliegel, M., and Cullati, S. (2019). Advantaged socioeconomic conditions in childhood are associated with higher cognitive functioning but strong cognitive decline in older age. *Proceedings of the National Academy of Sciences*, 116(2):5478–5486.
- Bai, R., Boland, M. R., and Chen, Y. (2019). Fast algorithms and theory for high-dimensional Bayesian varying coefficient models. *arXiv preprint arXiv:1907.06477*.
- Balocchi, C., Deshpande, S. K., George, E. I., and Jensen, S. T. (2023). Crime in Philadelphia: Bayesian clustering with particle optimization. *Journal of the American Statistical Association*, 118(542):818–829.
- Balocchi, C., George, E. I., and Jensen, S. T. (2021). Clustering areal units at multiple levels of resolution to model crime incidence in Philadelphia. *arXiv preprint arXiv:2112.02059*.
- Balocchi, C. and Jensen, S. T. (2019). Spatial modeling of trends in crime over time in Philadelphia. *Annals of Applied Statistics*, 13(4):2235–2259.
- Barbieri, M. M. and Berger, J. O. (2004). Optimal predictive model selection. *Annals of Statistics*, 32(3):870–897.
- Bürgin, R. and Ritschard, G. (2015). Tree-based varying coefficient regression for longitudinal ordinal responses. *Computational Statistics and Data Analysis*, 86:65–80.
- Bürgin, R. and Ritschard, G. (2017). Coefficient-wise tree-based varying coefficient regression with vcrpart. *Journal of Statistical Software*, 80(6):1–33.
- Center for High Throughput Computing (2006). Center for high throughput computing.
- Chipman, H. A., George, E. I., and McCulloch, R. E. (2010). BART: Bayesian Additive Regression Trees. *Annals of Applied Statistics*, 4(1):266–298.
- Chipman, H. A., George, E. I., McCulloch, R. E., and Shively, T. S. (2022). mbart: Multidimensional monotone BART. *Bayesian Analysis*, 17(2):515–544.
- Deshpande, S. K. (2023). **flexBART**: Flexible bayesian regression trees with categorical predictors. *arXiv preprint arXiv:2211.04459*.
- Dupre, M. E. (2007). Educational differences in age-related patterns of disease: Reconsidering the cumulative disadvantage and age-as-leveler hypotheses. *Journal of Health and Social Behavior*, 48(1):1–15.
- Eddelbuettel, D. and François, R. (2011). Rcpp: Seamless R and C++ integration. *Journal of Statistical Software*, 40(8):1 – 18.
- Eddelbuettel, D. and Sanderson, C. (2014). RcppArmadillo: Accelerating R with high-performance C++ linear algebra. *Computational Statistics and Data Analysis*, 71:1054 – 1063.

- Fan, J. and Zhang, W. (2008). Statistical methods with varying coefficient models. *Statistics and its Interface*, 1:179–195.
- Finley, A. O. and Banerjee, S. (2020). Bayesian spatially varying coefficient models in the spBayes R package. *Environmental Modelling and Software*, 125.
- Franco-Villoria, M., Ventrucci, M., and Rue, H. (2019). A unified view on Bayesian varying coefficient models. *Electronic Journal of Statistics*, 13(2):5334–5359.
- Gelfand, A. E., Kim, H.-J., Sirmans, C., and Banerjee, S. (2003). Spatial modeling with spatially varying coefficient processes. *Journal of the American Statistical Association*, 98(462):387–396.
- Ghosal, S. and van der Vaart, A. (2017). *Fundamentals of Nonparametric Bayesian Infernce*. Cambridge University Press.
- Greenfield, E. A. and Moorman, S. M. (2019). Childhood socioeconomic status and later life cognition: Evidence from the Wisconsin Longitudinal Study. *Journal of Aging and Health*, 31(9):1589–1615.
- Guhaniyogi, R., Li, C., Savitsky, T. D., and Srivastava, S. (2022). Distributed Bayesian varying coefficient modeling using a Gaussian process prior. *Journal of Machine Learning Research*, 23(84):1–59.
- Hahn, P. R., Murray, J. S., and Carvalho, C. M. (2020). Bayesian regression models for causal inference: regularization, confounding, and heterogeneous effects. *Bayesian Analysis*, 15(3):965–1056.
- Hastie, T. and Tibshirani, R. (1993). Varying-coefficient models. *Journal of the Royal Statistical Society Series B: Statistical Methodology*, 55(4):757–796.
- Hayfield, T. and Racine, J. S. (2008). Nonparametric econometrics: The np package. *Journal of Statistical Software*, 27(5).
- He, J., Yalov, S., and Hahn, P. R. (2019). XBART: Accelerated Bayesian Additive Regression Trees. In *Proceedings of Machine Learning Research*. PMLR.
- Hill, J. L. (2011). Bayesian nonparametric modeling for causal inference. *Journal of Computational and Graphical Statistics*, 20(1):217–240.
- Hill, J. L., Linero, A. R., and Murray, J. S. (2020). Bayesian Additive Regression Trees: A review and look forward. *Annual Review of Statistics and its Applications*, 7(1):251–278.
- Hoover, D. R., Rice, J. A., Wu, C. O., and Yang, L.-P. (1998). Nonparametric smoothing estimates of time-varying coefficient models with longitudinal data. *Biometrika*, 85(4):809–822.
- Huang, J. Z. and Shen, H. (2004). Functional coefficient regression models for non-linear time series: A polynomial splines approach. *Scandinavian Journal of Statistics*, 31:515–534.
- Huang, J. Z., Wu, C. O., and Zhou, L. (2002). Varying-coefficient models and basis function approximations for the analysis of repeated measurements. *Biometrika*, 89(1):111–128.
- Kim, J. and Ročková, V. (2023). On mixing rates for Bayesian CART. *arXiv preprint arXiv:2306.00126*.
- Krantsevich, N., He, J., and Hahn, P. R. (2021). Stochastic tree ensembles for estimating heterogeneous effects. In *Proceedings of the 38th International Conference on Machine Learning*. PMLR.
- Lee, K., Lee, Y. K., Park, B. U., and Yang, S. J. (2018). Time-dynamic varying coefficient models for longitudinal data. *Computational Statistics and Data Analysis*, 123:50–65.

- Li, Q. and Racine, J. S. (2010). Smooth varying-coefficient estimation and inference for qualitative and quantitative data. *Econometric Theory*, 26(6):1607–1637.
- Linero, A. R. (2018). Bayesian regression trees for high-dimensional prediction and variable selection. *Journal of the American Statistical Association*, 113(522):626–636.
- Linero, A. R., Sinha, D., and Lipsitz, S. R. (2020). Semiparametric mixed-scale models using shared Bayesian forests. *Biometrics*, 76(1):131–144.
- Linero, A. R. and Yang, Y. (2018). Bayesian regression tree ensembles that adapt to smoothness and sparsity. *Journal of the Royal Statistical Society Series B: Statistical Methodology*, 80(5):1087–1110.
- Luo, Y. and Waite, L. J. (2005). The impacts of childhood and adult SES on physical, mental, and cognitive well-being in later life. *The Journals of Gerontology: Series B*, 60(2):S93–S101.
- Lyu, J. and Burr, J. (2016). Socioeconomic status across the life course and cognitive function among older adults: An examination of the latency, pathways, and accumulate hypotheses. *Journal of Aging Health*, 28(1):40–67.
- Marden, J., Tchetgen Tchetgen, E. J., Kawachi, I., and Glymour, M. (2017). Contribution of socioeconomic status and 3 life-course periods to late-life memory function and decline: early and late predictors of dementia risk. *American Journal of Epidemiology*, 186(7):805–814.
- McCulloch, R., Sparapani, R., Gramacy, R., Spanbauer, C., and Pratola, M. (2018). **BART: Bayesian Additive Regression Trees**. R package version 2.1.
- Murray, J. S. (2021). Log-linear Bayesian additive regression trees for categorical and count responses. *Journal of the American Statistical Association*, 116(534):756–769.
- R Core Team (2019). *R: A language and environment for statistical computing*. R Foundation for Statistical Computing, Vienna, Austria.
- Roberts, G. O. and Rosenthal, J. S. (2009). Examples of adaptive MCMC. *Journal of Computational and Graphical Statistics*, 18(2):349–367.
- Ronen, O., Saarinen, T., Tan, Y. S., Duncan, J., and Yu, B. (2022). A mixing time lower bound for a simplified version of BART. *arXiv preprint arXiv:2210.09352v1*.
- Ročková, V. and George, E. I. (2014). EMVS: The EM approach to Bayesian variable selection. *Journal of the American Statistical Association*, 109(506):828–846.
- Ročková, V. and Saha, E. (2019). On theory for BART. In *Proceedings of the 22nd International Conference on Artificial Intelligence and Statistics*, pages 2839–2848.
- Ročková, V. and van der Pas, S. (2020). Posterior concentration for Bayesian regression trees and forests. *Annals of Statistics*, 48(4):2108–2131.
- Sonnega, A., Faul, J., Ofstedal, M., Langa, K. M., Phillips, J. W., and Weir, D. R. (2014). Cohort profile: The Health and Retirement Study (HRS). *International Journal of Epidemiology*, 43(2):576–585.
- Sparapani, R., Logan, B. R., McCulloch, R. E., and Laud, P. W. (2016). Nonparametric survival analysis using Bayesian Additive Regression Trees. *Statistics in Medicine*, 35(16):2741–2753.
- Starling, J. E., Aiken, C. E., Murray, J. S., Nakimuli, A., and Scott, J. G. (2019). Monotone function estimation in the presence of extreme data coarsening: Analysis of preeclampsia and birth weight in urban Uganda. *arXiv preprint arXiv:1912.06946*.

- Starling, J. E., Murray, J. S., Carvalho, C. M., Bukowski, R., and Scott, J. G. (2020). BART with targeted smoothing: An analysis of patient-specific stillbirth risk. *Annals of Applied Statistics*, 14(1):28–50.
- Tan, Y. V. and Roy, J. (2019). Bayesian Additive Regression Trees and the General BART model. *Statistics in Medicine*, 38(25):5048–5069.
- Tibshirani, R. and Friedman, J. (2020). A pliable lasso. *Journal of Computational and Graphical Statistics*, 29(1):215–225.
- Vable, A. M., Gilsanz, P., Nguyen, T. T., Kawachi, I., and Glymour, M. M. (2017). Validation of a theoretically motivated approach to measuring childhood socioeconomic circumstances in the Health and Retirement Study. *PLoS ONE*, 12(10):e0185898.
- Wang, H. and Xia, Y. (2009). Shrinkage estimation for the varying coefficient model. *Journal of the American Statistical Association*, 104(486):747–757.
- Wang, J. C. and Hastie, T. (2012). Boosted varying-coefficient regression models for product demand prediction. *Journal of Computational and Graphical Statistics*, 23(2):361–382.
- Wang, L., Li, H., and Huang, J. Z. (2008). Variable selection in nonparametric varying-coefficient models for analysis of repeated measurements. *Journal of the American Statistical Association*, 103(484):1556–1569.
- Wei, F., Huang, J., and Li, H. (2011). Variable selection and estimation in high-dimensional varying-coefficient models. *Statistica Sinica*, 21:1515–1540.
- Woody, S., Carvalho, C. M., Hahn, P. R., and Murray, J. S. (2020). Estimating heterogeneous effects of continuous exposures using Bayesian tree ensembles: Revising the impact of abortion rates on crime. *arXiv preprint arXiv:2007.09845v1*.
- Wright, M. N. and Ziegler, A. (2017). ranger: A fast implementation of random forests for high dimensional data in C++ and R. *Journal of Statistical Software*, 77(1):1–17.
- Wu, C. O. and Chiang, C.-T. (2000). Kernel smoothing on varying coefficient models with longitudinal dependent variable. *Statistica Sinica*, 10:433–456.
- Xu, D., Daniels, M. J., and Winterstein, A. G. (2016). Sequential BART for imputation of missing covariates. *Biostatistics*, 17(3):589–602.
- Zhang, Z., Liu, H., and Choi, S.-w. (2020). Early-life socioeconomic status, adolescent cognitive ability, and cognition in late midlife: Evidence from the Wisconsin Longitudinal Study. *Social Science & Medicine*, 244:112575.
- Zhou, Y. and Hooker, G. (2022). Decision tree boosted varying coefficient models. *Data Mining and Knowledge Discovery*, 36:2237–2271.

Supplementary Materials

S1 Proofs of asymptotic results

S1.1 Notation and Preliminaries

The proof of Theorem 1 is based on the standard prior concentration and testing arguments outlined in Ghosal and van der Vaart (2017). Roughly speaking, in order to prove optimal posterior concentration, the prior on $\beta = [\beta_0, \dots, \beta_p]$ first needs to be “close” enough to β_0 (i.e. the prior needs to assign enough positive probability mass to a neighborhood of β_0). Second, we need to construct exponentially powerful statistical tests, so that the probabilities of Type I and Type II errors for testing $H_0 : \beta = \beta_0$ vs. $H_1 : \{\|\beta - \beta_0\|_n > r_n\}$ are exponentially decreasing.

Throughout this section, we use the following notation. For two nonnegative sequences $\{a_n\}$ and $\{b_n\}$, we write $a_n \asymp b_n$ to denote $0 < \liminf_{n \rightarrow \infty} a_n/b_n \leq \limsup_{n \rightarrow \infty} a_n/b_n < \infty$. If $\lim_{n \rightarrow \infty} a_n/b_n = 0$, we write $a_n = o(b_n)$ or $a_n \prec b_n$. We use $a_n \lesssim b_n$ or $a_n = O(b_n)$ to denote that for sufficiently large n , there exists a constant $C > 0$ independent of n such that $a_n \leq Cb_n$. For a function β , $\|\beta\|_\infty = \max_{z \in [0,1]^R} |\beta(z)|$. Finally, for a symmetric matrix \mathbf{A} , we let $\lambda_{\min}(\mathbf{A})$ and $\lambda_{\max}(\mathbf{A})$ denote its minimum and maximum eigenvalues

For two densities f and g , let $K(f, g) = \int f \log(f/g)$ and $V(f, g) = \int f |\log(f/g) - K(f/g)|^2$ denote the Kullback-Leibler (KL) divergence and KL variation respectively. Denote the Rényi divergence of order $1/2$ as $\rho(f, g) = -\log \int f^{1/2} g^{1/2} d\nu$. Finally, denote the ε -covering number for a set Ω with semimetric d as the minimum number of d -balls of radius ε needed to cover Ω and denote the ε -covering number as $N(\varepsilon, \Omega, d)$ and the metric entropy as $\log N(\varepsilon, \Omega, d)$.

To prove near-optimal posterior concentration for VCBART, we need to make the following assumptions. Below, we let $\alpha_{\min} := \min\{\alpha_0, \dots, \alpha_p\}$ and $n_{\max} = \max\{n_1, \dots, n_n\}$.

(A1) $\|\beta_{0,j}\|_\infty < \infty$ for $0 \leq j \leq p$.

(A2) There exists a constant $D > 0$ so that $|x_{itj}| \leq D$ for all $1 \leq i \leq n, 1 \leq t \leq n_i, 1 \leq j \leq p$.

(A3) $p = o(N^{2\alpha_{\min}/(2\alpha_{\min}+R)}/\log N)$, $R = O((\log N)^{1/2})$, and $n_{\max} \asymp N/n$.

(A4) The eigenvalues of each within-subject correlation matrix Σ_i satisfy

$$1 \lesssim \min_{1 \leq i \leq n} \lambda_{\min}(\Sigma_i(\rho_0)) \leq \max_{1 \leq i \leq n} \lambda_{\max}(\Sigma_i(\rho_0)) \lesssim 1,$$

and for any $(\sigma_1^2, \rho_1), (\sigma_2^2, \rho_2) \in (0, \infty) \times (0, 1)$

$$\begin{aligned} \max_{1 \leq i \leq n} \|\sigma_1^2 \Sigma_i(\rho_1) - \sigma_2^2 \Sigma_i(\rho_2)\|_F^2 &\leq \frac{1}{n} \|\sigma_1^2 \Sigma(\rho_1) - \sigma_2^2 \Sigma(\rho_2)\|_F^2 \\ &\lesssim n_{\max}^2 (\sigma_1^2 - \sigma_2^2)^2 + n_{\max}^4 \sigma_2^2 |\rho_1 - \rho_2|^2. \end{aligned}$$

where $\Sigma = \text{diag}(\Sigma_1, \dots, \Sigma_n)$.

Assumption (A1) requires the true $\beta_{0,j}$'s to be uniformly bounded. Since the effect modifiers \mathbf{z} have been rescaled to lie in $[0, 1]^R$, this assumption is likely to be satisfied in practice. Assumption (A2) requires that the covariates x_{itj} are uniformly bounded for all i, t, j . Assumption (A3) allows the number of covariates p to diverge to infinity but at a slower rate than N . This assumption is needed to ensure that the contraction rate converges to zero as $n, p \rightarrow \infty$. Assumption (A3) also allows the number of effect modifiers R to grow with n , but at a much slower rate. Assumption (A4) assumes that the within-subject correlation matrices are asymptotically well-behaved in the sense that the eigenvalues for every Σ_i are bounded away from zero and infinity, and the maximum squared Frobenius norm for the difference between any two correlation matrices of size $n_i \times n_i$ is bounded above by a function of n_{\max} . Many commonly used correlation structures like first-order autoregressive, compound symmetry, and moving average satisfy this assumption.

S1.2 Proof of Theorem 1

Let $\theta_{it} = \sum_{j=0}^p \beta_{0,j}(\mathbf{z}_{it}) x_{itj}$, and let $\boldsymbol{\theta}_i = (\theta_{i1}, \dots, \theta_{in_i})^\top$ denote the $n_i \times 1$ vector corresponding to the i th subject. Let $\boldsymbol{\theta} = (\boldsymbol{\theta}_1^\top, \dots, \boldsymbol{\theta}_n^\top)^\top$ be the $N \times 1$ vector of all the θ_{it} 's. Let $\theta_{0,itj} = \sum_{j=0}^p \beta_{0,j}(\mathbf{z}_{it}) x_{itj}$ and define $\boldsymbol{\theta}_{0,i} = (\theta_{0,i1}, \dots, \theta_{0,in_i})^\top$ and $\boldsymbol{\theta}_0 = (\boldsymbol{\theta}_{0,1}^\top, \dots, \boldsymbol{\theta}_{0,n}^\top)^\top$. Let $\mathbb{P}_{\boldsymbol{\beta}_0}^{(N)}$ denote the probability measure underlying the true model,

$$y_{it} = \beta_{0,0}(\mathbf{z}_{it}) + \sum_{j=0}^p \beta_{0,j}(\mathbf{z}_{it}) x_{itj} + \sigma_0 \varepsilon_{it}, \quad 1 \leq i \leq n, 1 \leq t \leq n_i, \quad (\text{S1})$$

where $\boldsymbol{\varepsilon}_i = (\varepsilon_{i1}, \dots, \varepsilon_{in_i})' \stackrel{\text{ind}}{\sim} \mathcal{N}_{n_i}(\mathbf{0}_{n_i}, \Sigma_i(\rho_0))$, $\rho_0 \in [0, 1]$. Recall that $N = \sum_{i=1}^n n_i$ is the total number of observations. For the i th observation, the response $\mathbf{y}_i = (y_{i1}, \dots, y_{in_i})^\top$ is distributed as $\mathbf{y}_i \sim \mathcal{N}_{n_i}(\boldsymbol{\theta}_i, \sigma^2 \Sigma_i(\rho_0))$. Let f_i denote the density for \mathbf{y}_i and $f = \prod_{i=1}^n f_i$. Analogously, the let $f_{0,i}$ be the density for $\mathbf{y}_i \sim \mathcal{N}_{n_i}(\boldsymbol{\theta}_{0,i}, \sigma^2 \Sigma_i(\rho_0))$, and let $f_0 = \prod_{i=1}^n f_{0,i}$.

The proof of Theorem 1 can be sketched as follows. First we establish the optimal *prior* concentration for the VCBART prior in Lemma 2 and the optimal posterior contraction with respect to average Rényi divergence of order 1/2 in Lemma 3. This will then imply the optimal posterior contraction in the empirical ℓ_2 norm.

Lemma 2. *Under (S1), suppose we endow $(\boldsymbol{\beta}, \sigma)$ with the VCBART prior and the autoregressive*

parameter ρ with the uniform prior, $\rho \sim \mathcal{U}(0, 1)$. For the BART priors on the β_j 's, $j = 0, \dots, p$, suppose that the splitting probability of a node is $q(d) = \gamma^d$ for some $1/N \leq \gamma < 1/2$ and that the splitting indices are chosen uniformly (i.e. $\boldsymbol{\theta} = (1/R, \dots, 1/R)$). For the half- t_ν prior on σ , assume $\nu > 1$. Assume that Assumptions (A1)-(A4) hold. Then for $r_N^2 = \log N \sum_{j=0}^p N^{-2\alpha_j/(2\alpha_j+R)}$ and some $C_1 > 0$,

$$\Pi(K(f_0, f) \leq nr_N^2, V(f_0, f) \leq Nr_N^2) \gtrsim \exp(-C_1 Nr_N^2). \quad (\text{S2})$$

Proof of Lemma 2. Our proof follows along the same lines as the proof of Lemma 1 in Bai et al. (2019), with suitable modifications for the fact that we use BART priors on the functionals $\boldsymbol{\beta}$. Denote $\boldsymbol{\Sigma}_i^* = (\sigma^2/\sigma_0^2)\boldsymbol{\Sigma}_{0i}^{-1/2}\boldsymbol{\Sigma}_i\boldsymbol{\Sigma}_{0i}^{-1/2}$, $i = 1, \dots, n$. Denote the ordered eigenvalues of $\boldsymbol{\Sigma}_i^*$ by λ_{it} , $1 \leq t \leq n_i$, and let $\boldsymbol{\Sigma}^* = \text{diag}(\boldsymbol{\Sigma}_1^*, \dots, \boldsymbol{\Sigma}_n^*)$. Noting that the n subjects are independent, we have

$$\begin{aligned} K(f_0, f) &= \frac{1}{2} \left\{ \sum_{i=1}^n \sum_{t=1}^{n_i} (\lambda_{it} - 1 - \log \lambda_{it}) + \frac{\|\boldsymbol{\Sigma}^{-1/2}(\boldsymbol{\theta} - \boldsymbol{\theta}_0)\|_2^2}{\sigma^2} \right\}, \\ V(f_0, f) &= \left[\sum_{i=1}^n \sum_{t=1}^{n_i} \frac{(1 - \lambda_{it})^2}{2} \right] + \frac{\sigma_0^2}{(\sigma^2)^2} \|\boldsymbol{\Sigma}_0^{1/2} \boldsymbol{\Sigma}^{-1}(\boldsymbol{\theta} - \boldsymbol{\theta}_0)\|_2^2. \end{aligned}$$

Define the sets,

$$\begin{aligned} \mathcal{A}_1 &= \left\{ \sigma : \sum_{i=1}^n \sum_{t=1}^{n_i} (\lambda_{it} - 1 - \log \lambda_{it}) \leq Nr_N^2, \sum_{i=1}^n \sum_{t=1}^{n_i} (1 - \lambda_{it})^2 \right\}, \\ \mathcal{A}_2 &= \left\{ (\boldsymbol{\beta}, \sigma) : \frac{\|\boldsymbol{\Sigma}^{-1/2}(\boldsymbol{\theta} - \boldsymbol{\theta}_0)\|_2^2}{\sigma^2} \leq Nr_N^2, \frac{\sigma_0^2}{(\sigma^2)^2} \|\boldsymbol{\Sigma}_0^{1/2} \boldsymbol{\Sigma}^{-1}(\boldsymbol{\theta} - \boldsymbol{\theta}_0)\|_2^2 \leq \frac{Nr_N^2}{2} \right\}. \end{aligned}$$

Then $\Pi(K(f_0, f) \leq Nr_N^2, V(f_0, f) \leq Nr_N^2) = \Pi(\mathcal{A}_2|\mathcal{A}_1)\Pi(\mathcal{A}_1)$, and so we can consider $\Pi(\mathcal{A}_2|\mathcal{A}_1)$ separately. Using almost identical arguments as those in the proof of Lemma 1 of Bai et al. (2019),

$$\Pi(\mathcal{A}_1) \gtrsim \exp(-C_1 Nr_N^2/2), \quad (\text{S3})$$

for some $C_1 > 0$. Next we focus on bounding $\Pi(\mathcal{A}_2|\mathcal{A}_1)$ from below. Similarly as in the proof of Lemma 1 of Bai et al. (2019), the left-hand side for both inequalities in the set \mathcal{A}_2 , conditional on \mathcal{A}_1 , can be bounded above by a constant multiple of $\|\boldsymbol{\theta} - \boldsymbol{\theta}_0\|_2^2$. Thus, for some constant $b_1 > 0$,

we have as a lower bound for $\Pi(\mathcal{A}_2|\mathcal{A}_1)$,

$$\begin{aligned}
\Pi(\mathcal{A}_2|\mathcal{A}_1) &\geq \Pi\left(\beta : \|\theta - \theta_0\|_2^2 \leq \frac{Nr_N^2}{2b_1}\right) \\
&= \Pi\left(\beta : \sum_{i=1}^n \sum_{t=1}^{n_i} \left[\sum_{j=0}^p \beta_j(\mathbf{z}_{it})x_{ij} - \sum_{j=0}^p \beta_{0,j}(\mathbf{z}_{it})x_{ij} \right]^2 \leq \frac{Nr_N^2}{2b_1}\right) \\
&\geq \Pi\left(\beta : \sum_{i=1}^n \sum_{t=1}^{n_i} \sum_{j=0}^p [\beta_j(\mathbf{z}_{it}) - \beta_{0,j}(\mathbf{z}_{it})]^2 \leq \frac{Nr_N^2}{2b_1 D^2(p+1)}\right) \\
&\geq \prod_{j=0}^p \Pi\left(\beta_j : \sum_{i=1}^n \sum_{t=1}^{n_i} [\beta_j(\mathbf{z}_{it}) - \beta_{0,j}(\mathbf{z}_{it})]^2 \leq \frac{N(r_N^j)^2}{2b_1 D^2(p+1)}\right) \\
&\geq \prod_{j=0}^p \Pi\left(\beta_j : \|\beta_j - \beta_{0,j}\|_N \leq \frac{r_N^j}{D_2 \sqrt{2b_1(p+1)}}\right), \tag{S4}
\end{aligned}$$

where $r_N^j = N^{-\alpha_j/(2\alpha_j+R)} \log^{1/2} N$, $j = 0, \dots, p$, and we used Assumption (A2) about the uniform boundedness of the covariates and an application of the Cauchy-Schwarz inequality in the third line of the display. Since we want to show that $\Pi(\mathcal{A}_2|\mathcal{A}_1) \gtrsim \exp(-C_1 N r_N^2/2)$, it suffices to show (based on the last line of (S4)) that for each function β_j , $j = 0, \dots, p$,

$$\Pi\left(\beta_j : \|\beta_j - \beta_{0,j}\|_N \leq \frac{r_N^j}{D_2 \sqrt{2b_1(p+1)}}\right) \gtrsim e^{-C_1 N (r_N^j)^2/2}. \tag{S5}$$

Note that the lower bound in (S5) holds due to Assumption (A1) that $\|\beta_{0,j}\|_\infty \prec \log^{1/2} N$ for all $1 \leq j \leq p$, Assumption (A3) that $R = O((\log N)^{1/2})$, and the proof of Theorem 7.1 of Ročková and Saha (2019). Thus, from (S4)-(S5), we have that $\Pi(\mathcal{A}_2|\mathcal{A}_1)$ is lower bounded by $\exp(-C_1 N r_N^2)$. Combined with (S3), this yields the desired lower bound in (S2). \square

Next, we prove posterior contraction of f to the truth f_0 with respect to average Rényi divergence of order $1/2$.

Lemma 3. *Under (S1), suppose we endow (β, σ) with the VCBART prior and the autoregressive parameter ρ with the uniform prior, $\rho \sim \mathcal{U}(0, 1)$. For the BART priors on the β_j 's, $j = 0, \dots, p$, suppose that the splitting probability of a node is $q(d) = \gamma^d$ for some $1/N \leq \gamma < 1/2$ and that the splitting indices are chosen uniformly (i.e. $\theta = (1/R, \dots, 1/R)$). For the half- t_ν prior on σ , assume $\nu > 1$. Assume that Assumptions (A1)-(A4) hold. Then for $r_N^2 = \log N \sum_{j=0}^p N^{-2\alpha_j/(2\alpha_j+R)}$ and some $C_2 > 0$,*

$$\Pi\left(\frac{1}{N} \rho(f, f_0) \geq C_2 r_N^2 | \mathbf{Y}\right) \rightarrow 0, \tag{S6}$$

in $\mathbb{P}_{f_0}^{(N)}$ probability as $N, p \rightarrow \infty$.

Proof of Lemma 3. This statement will be proven if we can establish that for some $C_1, C_3 > 0$,

$$\Pi(K(f_0, f) \leq Nr_N^2, V(f_0, f) \leq Nr_N^2) \gtrsim \exp(-C_1 Nr_N^2), \quad (\text{S7})$$

as well as the existence of a sieve $\{\mathcal{F}_N\}_{N=1}^\infty$ such that

$$\Pi(\mathcal{F}_N^c) \leq \exp(-C_3 Nr_N^2), \quad (\text{S8})$$

and a test function φ_n such that

$$\begin{aligned} \mathbb{E}_{f_0} \varphi_N &\leq e^{-Nr_N^2}, \\ \sup_{f \in \mathcal{F}_N: \rho(f, f_0) > C_2 Nr_N^2} \mathbb{E}_f(1 - \varphi_N) &\lesssim e^{-Nr_N^2/16}. \end{aligned} \quad (\text{S9})$$

We already proved (S7) in Lemma 2. To verify (S8), we consider the sieve,

$$\mathcal{F}_n = \left\{ (\beta, \sigma, \rho) : 0 < \sigma < e^{C_4 Nr_N^2}, e^{-C_4 Nr_N^2} < \rho < 1 - e^{-C_4 Nr_N^2}, \beta_j \in \mathcal{B}_N^j, j = 0, \dots, p \right\},$$

where for each $j = 0, \dots, p$, \mathcal{B}_N^j is defined as the sieve in the proof of Theorem 7.1 of Ročková and Saha (2019), i.e. the union of all functions belonging to the class of functions \mathcal{F}_ε (defined in Ročková and van der Pas (2020)) that are supported on a valid ensemble \mathcal{VE} (Ročková and van der Pas, 2020), where *each* tree in the j th ensemble \mathcal{E}_j has at most l_N^j leaves, and l_N^j is chosen as $l_N^j = \lfloor \tilde{D}N(r_N^j)^2 / \log N \rfloor \asymp N^{R/(2\alpha_j + R)}$, for sufficiently large $\tilde{D} > 0$. With this choice of sieve, we have

$$\Pi(\mathcal{F}_n^c) \leq \Pi(\sigma > e^{C_4 Nr_N^2}) + \Pi(\rho \leq e^{-C_4 Nr_N^2}) + \Pi(\rho \geq 1 - e^{-C_4 Nr_N^2}) + \sum_{j=0}^p \Pi(\beta_j \notin \mathcal{B}_n^j). \quad (\text{S10})$$

Since we assumed that $\nu > 1$ in the half- t_ν prior on σ , $\mathbb{E}(\sigma)$ is well-defined, and a simple application of the Markov inequality gives $\Pi(\sigma > e^{C_4 Nr_N^2}) \leq e^{-C_4 Nr_N^2} \mathbb{E}(\sigma) \lesssim e^{-C_5 Nr_N^2}$ for some $C_5 > 0$. Obviously, the second and third terms in (S10) are each equal to $e^{-C_4 Nr_N^2}$, since $\rho \sim \mathcal{U}(0, 1)$.

We now focus on bounding the final term in (S10) from above. Let L_m^j denote the number of terminal leaf nodes in the m th tree of the j th tree ensemble \mathcal{E}_j corresponding to the functional $\beta_j(z)$. Let $l_N^{\min} = \min\{l_N^1, \dots, l_N^p\}$, recalling $l_N^j = \lfloor \tilde{D}N(r_N^j)^2 / \log N \rfloor$. Noting that all the BART priors have the same number of trees M , we have that the second term in (S10) can be bounded

above as

$$\begin{aligned}
\sum_{j=0}^p \Pi(\beta_j \notin \mathcal{B}_n^j) &\leq \sum_{j=0}^p \Pi\left(\bigcup_{m=1}^M \{L_m^j > l_N^j\}\right) \\
&\leq \sum_{j=0}^p \sum_{m=1}^M \Pi(L_m^j > l_N^j) \\
&\lesssim M \sum_{j=0}^p e^{-C_l l_N^j \log l_N^j} \\
&\lesssim Mp \exp(-C_l l_N^{\min} \log l_N^{\min}) \\
&= M \exp(\log p - C_l l_N^{\min} \log l_N^{\min}), \tag{S11}
\end{aligned}$$

where we used the proof of Theorem 7.1 of Ročková and Saha (2019) for the third line. By our assumption on the growth rate of p in Assumption (A3), we have $Me^{-C_l l_N^{\min} \log l_N^{\min} + \log p + C_5 N r_N^2} \rightarrow 0$ as $N, p \rightarrow \infty$ for sufficiently large $C_l > 0$ and any $C_5 > 0$. Thus, we have from (S11) that the final term on the right-hand side of (S10) is bounded above by $e^{-C_6 n r_N^2}$ for some $C_6 > 0$. Since each of the terms in (S10) can be bounded above by $e^{K N r_N^2}$ for some constant K , we see that (S8) holds.

Now we show the existence of a test function ϕ_N so that (S9) also holds. As in Bai et al. (2019), we first consider the most powerful Neyman-Pearson test $\phi_N = \mathbb{I}\{f_1/f_0 \geq 1\}$ for any f_1 such that $\rho(f_0, f_1) \geq N r_N^2$, where $f_1 = \prod_{i=1}^n f_{1,i}$ and $f_{1,i}$ is the density for $\mathbf{y}_i \sim \mathcal{N}_{n_i}(\boldsymbol{\theta}_{1,i}, \sigma_1^2 \boldsymbol{\Sigma}_i(\rho_1))$. If the average Rényi divergence between f_0 and f_1 is bigger than r_N^2 , then

$$\begin{aligned}
\mathbb{E}_{f_0} \phi_N &\leq e^{-N \varepsilon_N^2}, \\
\mathbb{E}_{f_1} (1 - \phi_N) &\leq e^{-N \varepsilon_N^2}. \tag{S12}
\end{aligned}$$

By the Cauchy-Schwarz inequality, we have

$$\mathbb{E}_f (1 - \phi_N) \leq \{\mathbb{E}_{f_1} (1 - \phi_N)\}^{1/2} \{\mathbb{E}_{f_1} (f/f_1)^2\}^{1/2}, \tag{S13}$$

and thus, following from the second inequality in (S12) and (S13), we can control the probability of Type II error properly if $\mathbb{E}_{f_1} (f/f_1)^2 \leq e^{7N r_N^2/8}$. Using Assumptions (A2) and (A4) and the same arguments as those in the proof of Lemma 2 in Bai et al. (2019), we have that $\mathbb{E}_{f_1} (f/f_1)^2$ is bounded above by $e^{7N r_N^2/8}$ for densities f_1 satisfying

$$\begin{aligned}
\|\boldsymbol{\theta} - \boldsymbol{\theta}_1\|_2^2 &\leq \frac{N r_N^2}{16}, \\
\frac{1}{n} \|\sigma^2 \boldsymbol{\Sigma}(\rho) - \sigma_1^2 \boldsymbol{\Sigma}(\rho_1)\|_F^2 &\leq \frac{r_N^4}{4n_{\max}^2}. \tag{S14}
\end{aligned}$$

Combining this with the second inequality in (S12) and (S13) gives

$$\mathbb{E}_f(1 - \phi_N) \lesssim e^{-Nr_N^2/16}.$$

Thus, we see from the first inequality in (S12) and the above inequality that the test φ_N satisfying (S9) is obtained as the maximum of all tests ϕ_N described above, for each piece required to cover the sieve. To complete the proof of (S9), we need to show that the metric entropy, $\log N(r_N, \mathcal{F}_N, \rho(\cdot))$, i.e. the logarithm of the maximum number of pieces needed to cover \mathcal{F}_N can be bounded above asymptotically by Nr_N^2 . By Assumption (A2), we have that $\frac{1}{N}\|\boldsymbol{\theta} - \boldsymbol{\theta}_1\|_2^2 \leq D_2^2(p+1) \sum_{j=0}^p \|\beta_j - \beta_{0j}\|_N^2$, and by Assumption (A4), the left-hand side of the second inequality in (S14) is bounded above by $n_{\max}^2(\sigma^2 - \sigma_1^2)^2 + e^{2C_4Nr_N^2}n_{\max}^4(\rho - \rho_1)^2$ on $\tilde{\mathcal{F}}_N$. Thus, for densities f_1 satisfying (S14), the metric entropy can be bounded above by

$$\begin{aligned} & \sum_{j=0}^p \log N \left(\frac{r_N}{4D_2\sqrt{p+1}}, \{\beta_j \in \mathcal{F}_N : \|\beta_j - \beta_{0,j}\|_N < r_N\}, \|\cdot\|_N \right) \\ & + \log N \left(\frac{r_N^2}{\sqrt{8}n_{\max}^2}, \{\sigma^2 : 0 < \sigma^2 < e^{C_4Nr_N^2}\}, |\cdot| \right) \\ & + \log N \left(\frac{r_N^2}{\sqrt{8}n_{\max}^3 e^{C_4Nr_N^2}}, \{\rho : 0 < \rho < 1\}, |\cdot| \right). \end{aligned} \quad (\text{S15})$$

One can easily verify that the last two terms in (S15) are upper bounded by a constant factor of Nr_N^2 . By modifying the proof of Theorem 7.1 in Ročková and Saha (2019) appropriately, we have for some $A_2 > 0$ and small $\delta > 0$ that the first term in (S15) can be upper bounded by

$$\sum_{j=0}^p \left[(l_N^j + 1)M \log(NRl_N^j) + A_2 M l_N^j \log \left(972D_2 \sqrt{M(p+1)l_N^j} N^{1+\delta/2} \right) \right], \quad (\text{S16})$$

where M is the number of trees in each ensemble \mathcal{B}_N^j . Recalling that M is fixed, $l_N^j \asymp N(r_N^j)^2 / \log N$ where $r_N^j = N^{-\alpha_j/(2\alpha_j+R)} \log^{1/2} N$, and Assumption (A3) that $R = O(\log^{1/2} N)$, we have that each summand in the first term in (S15) is upper bounded by $N(r_N^j)^2$, and so (S16) is asymptotically bounded above by $N \sum_{j=0}^p (r_N^j)^2 = Nr_N^2$. Therefore, from (S15)-(S16), we have for densities f_1 satisfying (S14),

$$\log N(r_N, \mathcal{F}_N, \rho(\cdot)) \lesssim Nr_N^2,$$

and so this completes the proof of (S9). Having established (S7)-(S9), it follows that we have posterior contraction with respect to average Rényi divergence, i.e. (S6) holds. \square

With Lemmas 2 and 3, we now have the ingredients to prove Theorem 1.

Proof of Theorem 1. By Lemma 3, $\Pi(N^{-1}\rho(f, f_0) \lesssim r_N^2 | \mathbf{Y}) \rightarrow 1$ in $\mathbb{P}_{f_0}^{(N)}$ -probability as $N, p \rightarrow \infty$, where $\rho(f_0, f)$ is the Rényi divergence of order 1/2. Under our assumptions and following similar arguments as those in the proof of Lemma 3 in Bai et al. (2019), posterior contraction w.r.t. average Rényi divergence then implies

$$\begin{aligned}
r_N^2 &\gtrsim \frac{1}{N} \|\boldsymbol{\theta} - \boldsymbol{\theta}_0\|_2^2 / (1 + r_N^2) \\
&= \frac{1}{N(1 + r_N^2)} \sum_{i=1}^n \sum_{t=1}^{n_i} \left[\sum_{j=0}^p [\beta_j(\mathbf{z}_{ij}) x_{itj} - \beta_{0,j}(\mathbf{z}_{ij}) x_{itj}] \right]^2 \\
&\gtrsim \frac{1}{N(1 + r_N^2)} \sum_{i=1}^n \sum_{t=1}^{n_i} \sum_{j=0}^p (\beta_j(\mathbf{z}_{ij}) - \beta_{0,j}(\mathbf{z}_{ij}))^2 \\
&\asymp \|\boldsymbol{\beta} - \boldsymbol{\beta}_0\|_N^2,
\end{aligned} \tag{S17}$$

where we used Assumption (A1) that $\|\beta_j\|_\infty < \infty$ for all $1 \leq j \leq p$ and Assumption (A2) that the covariates x_{itj} , $1 \leq i \leq n$, $1 \leq t \leq n_i$, $1 \leq j \leq p$, are uniformly bounded in the third line of the display. In the final line, we used the fact that $r_N^2 \rightarrow 0$ as $N \rightarrow \infty$. Thus, from (S17), the posterior is asymptotically supported on the event $\{\boldsymbol{\beta} : \|\boldsymbol{\beta} - \boldsymbol{\beta}_0\|_N^2 \leq M_2^2 r_N^2\}$ for sufficiently large N and some large constant $M_2 > 0$. This proves the theorem. \square

S2 Hyperparameter sensitivity

Recall from the main text, that each ensemble \mathcal{E}_j contained $M = 50$ trees and we set the prior jump variance $\tau_j = M^{-\frac{1}{2}}/2$. This induced a marginal $\mathcal{N}(0, 1/4)$ prior on each evaluation $\beta_j(\mathbf{z})$. Of course, if one has strong prior beliefs about the range of covariate effects, one can set τ_j in such a way that the implied marginal prior on $\beta_j(\mathbf{z})$ places substantial probability on this range. In this section, we consider the sensitivity of VCBART's covariance effect recovery and predictive capabilities to different choices of τ_j . Specifically, we replicate the synthetic data experiment from Section 4 of the main text with $N = 1,000$ total observations and vary $M \in \{50, 100, 200\}$ and $\tau_j = \tau/\sqrt{M}$ for $\tau \in \{0.25, 0.5, 1, 2, 4\}$.

Figures S7a and S7b are the analogs of Figures 3a and 3c of the main text, comparing the covariate effect recovery and predictive performance of VCBART with different values of (M, τ) . We observed that the coverages of posterior credible intervals for evaluations $\beta_j(\mathbf{z})$ and predictive intervals for testing outcomes were rather insensitive to both M and τ ; in fact, for each combination of M and τ the intervals all displayed much higher than nominal frequentist coverage. Figure S7c shows the F1 score for the median probability model for each combination of M and τ .

For each M , we see that as the covariate effect recovery and predictive performance degrades as

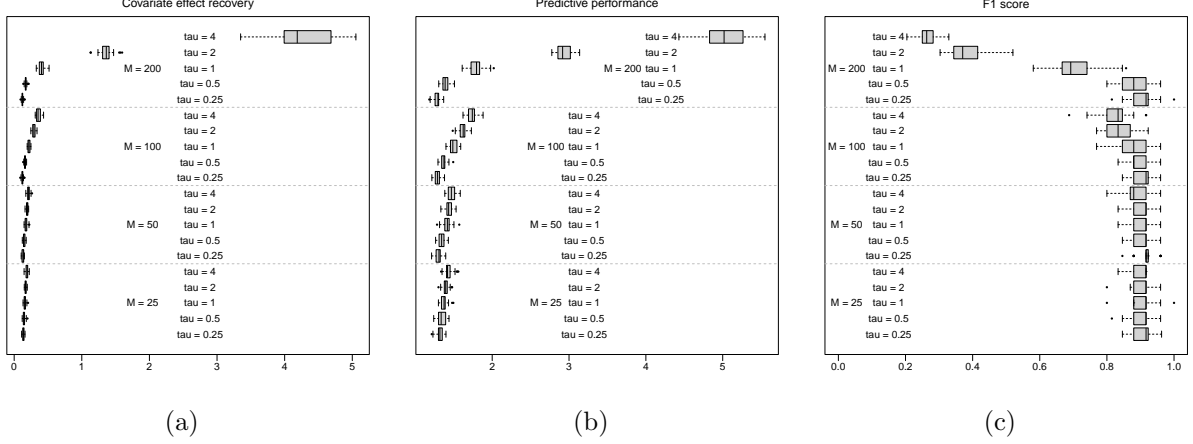


Figure S7: Covariate effect recovery, predictive, and modifier selection performance of VCBART run with different combinations of (M, τ_j) . (a) Total mean square error for estimating evaluations $\beta_j(\mathbf{z})$. (b) Predictive root mean square error. (c) F1 score of the median probability model. All measures reported over 25 testing datasets

we increase (resp. decrease) τ (resp. the amount of regularization). Interestingly, the degree to which performance degrades with increasing τ also increases with the total number of trees in the ensemble. Put differently, at least for our synthetic data generating process, VCBART’s performance is much more sensitive to τ when the number of trees M is large.

We further observed that the modifier selection performance of VCBART was much worse for $M = 200$ than it was for smaller ensemble sizes. On further inspection, we found that the estimated median probability model made too many false positive identifications in the supports of the $\beta_j(\mathbf{Z})$ ’s. That is, the tree ensembles \mathcal{E}_j split on too many spurious modifiers Z_r . We conjecture that the poor performance displayed in the top panel of Figure S7c is actually more general. Specifically, the combination of a too large ensemble size M and a Dirichlet prior on the vector of splitting probabilities will lead to a proliferation of false positives in the median probability model.

To develop some intuition about this conjecture, suppose that the function $\beta_j(\mathbf{Z})$ has been extremely well-approximated by the first $M' \ll M$ regression trees in an ensemble of size M . The Gibbs sampling underlying VCBART (and indeed, virtually all BART extensions), updates regression trees based on a partial residual based on the approximation provided by the other $M - 1$ trees. Once the sampler reaches the m -th tree with $m > M'$, the relevant partial residual will have very little variance. At this point, the tree is being used, essentially, to fit “noise,” with the first M' trees in the ensemble accounting for virtually all the “signal.” In this situation, spurious decision rules — that is, those based on modifiers that do not drive variation in $\beta_j(\mathbf{Z})$ — are not heavily penalized in the Metropolis-Hastings update. And once a split on a spurious variable has been accepted in a single MCMC iteration, the Dirichlet-Multinomial conjugacy underpinning our

decision rule prior, will encourage further splitting on that same variable, leading to a proliferation of false positive identifications. Introducing a dependence on M into our decision rule prior might alleviate this behavior. We leave such explorations for future work.

S3 Additional experimental results

S3.1 Implementation details

VCBART is implemented in C++ and interfaces with R (R Core Team, 2019) through **Rcpp** (Eddelbuettel and François, 2011) and **RcppArmadillo** Eddelbuettel and Sanderson (2014). Our implementation uses the basic class structures of **flexBART** (Deshpande, 2023). We have created an R package **VCBART**, which is available online at <https://github.com/skdeshpande91/VCBART>. We performed all of the experiments reported in Sections 4 and 5 of the main text on a high throughput computing cluster (Center for High Throughput Computing, 2006). All experiments were run in R version 4.1.3 on compute nodes with 10GB of RAM and AMD EPYC 7763 processors.

Where possible, we ran the competing methods in our simulations with package defaults and did not implement any additional tuning procedures. For instance, the default implementation of Zhou and Hooker (2022)’s boosted tree procedure (referred to as BTVM in Section 4.1 of the main text) does not automatically perform cross-validation to set the learning rate or number of boosting iterations. Instead, we ran BTVM for 200 iterations and with a learning rate of 0.5, which are the same settings as the example provided by the authors at <https://github.com/siriuz42/treeboostVCM>. Similarly the implementation of extremely randomized trees in the **ranger** package (Wright and Ziegler, 2017) does not automatically perform cross-validation to select the number of possible splitting variables at each node (i.e. the parameter `mtry`). In our experiments, we used the package default, setting `mtry` equal to the square root of the number of inputs.

S3.2 Function-by-function covariate recovery performance

Figure 2 of the main text plotted estimates of $\beta_0(\mathbf{z})$, $\beta_1(\mathbf{z})$, $\beta_2(\mathbf{z})$ and $\beta_3(\mathbf{z})$ computed after fitting a VCBART model to $N = 1000$ total observations. Figure S8 plots the posterior means of each $\beta_j(\mathbf{z})$ against the actual value. With the exception of Figure S8d, we see that the points fall close to the 45-degree line, indicating that our posterior mean estimates of $\beta_j(\mathbf{z})$ are close to the actual values used to generate the data. Recall that we generated the data with a constant $\beta_3(\mathbf{z}) = 1$ and with a residual standard deviation of $\sigma = 1$. On further inspection, we found that the vast majority of the estimated $\beta_3(\mathbf{z})$ ’s were within half a standard deviation of the true value $\beta_3(\mathbf{z}) = 1$. So although the VCBART estimates of the constant function were not constant, the estimated values were still quite close to the true function value.

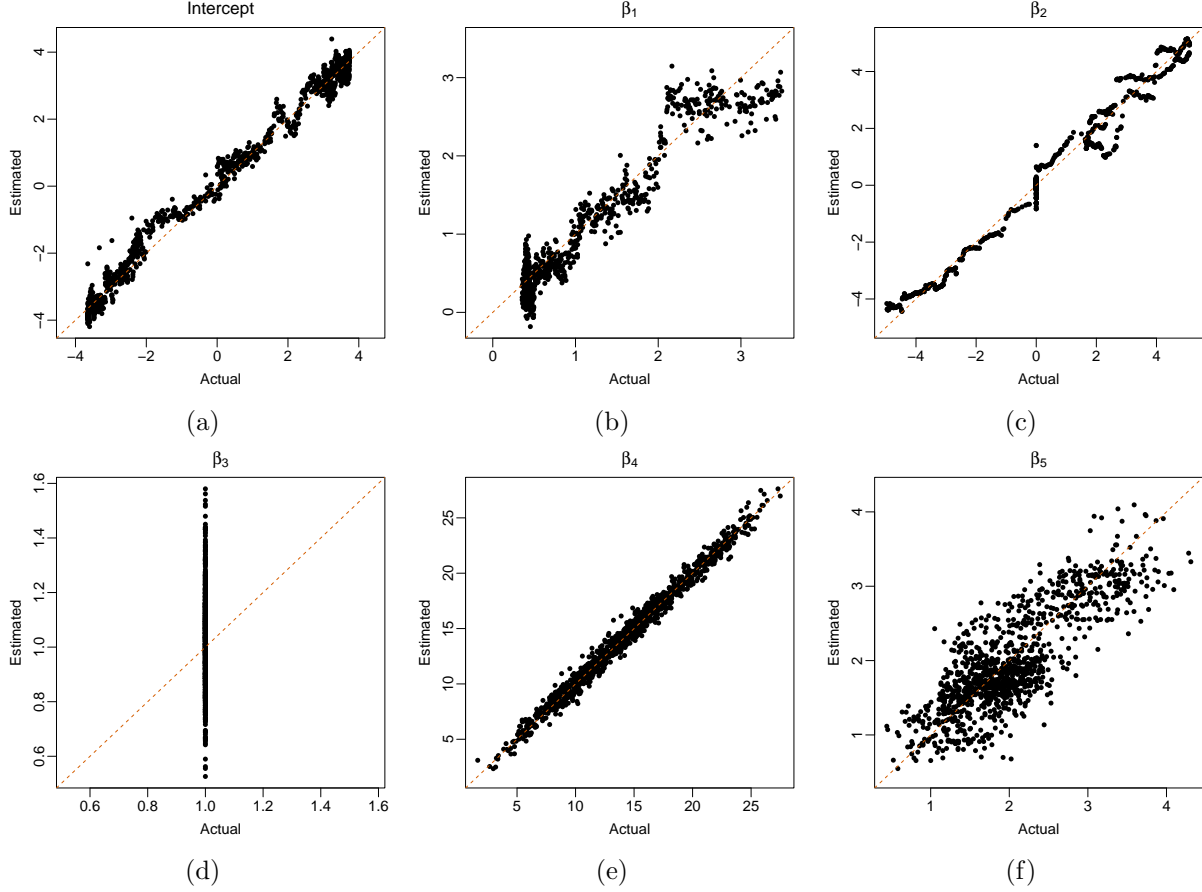


Figure S8: Actual and VCBART estimates of the $\beta_j(\mathbf{z})$ used to generate the data underpinning Figure 2 of the main text. For the non-constant functions $\beta_j(\mathbf{z})$ for $j \neq 3$, we see that the estimates are quite close to the actual values

Across the 25 training–testing splits considered in Section 4 of the main text, VCBART produced consistently more accurate estimates of each individual function β_j . Figures 3a and 3b in the main text compared the mean square error and uncertainty interval coverage of VCBART and several competitors averaged across all functions and test-set inputs. Figures S9 and S10 are analogs of those two figures that compare the function-by-function mean square and uncertainty interval coverage. We see that VCBART clearly outperforms the other competitors in terms of recovering each function.

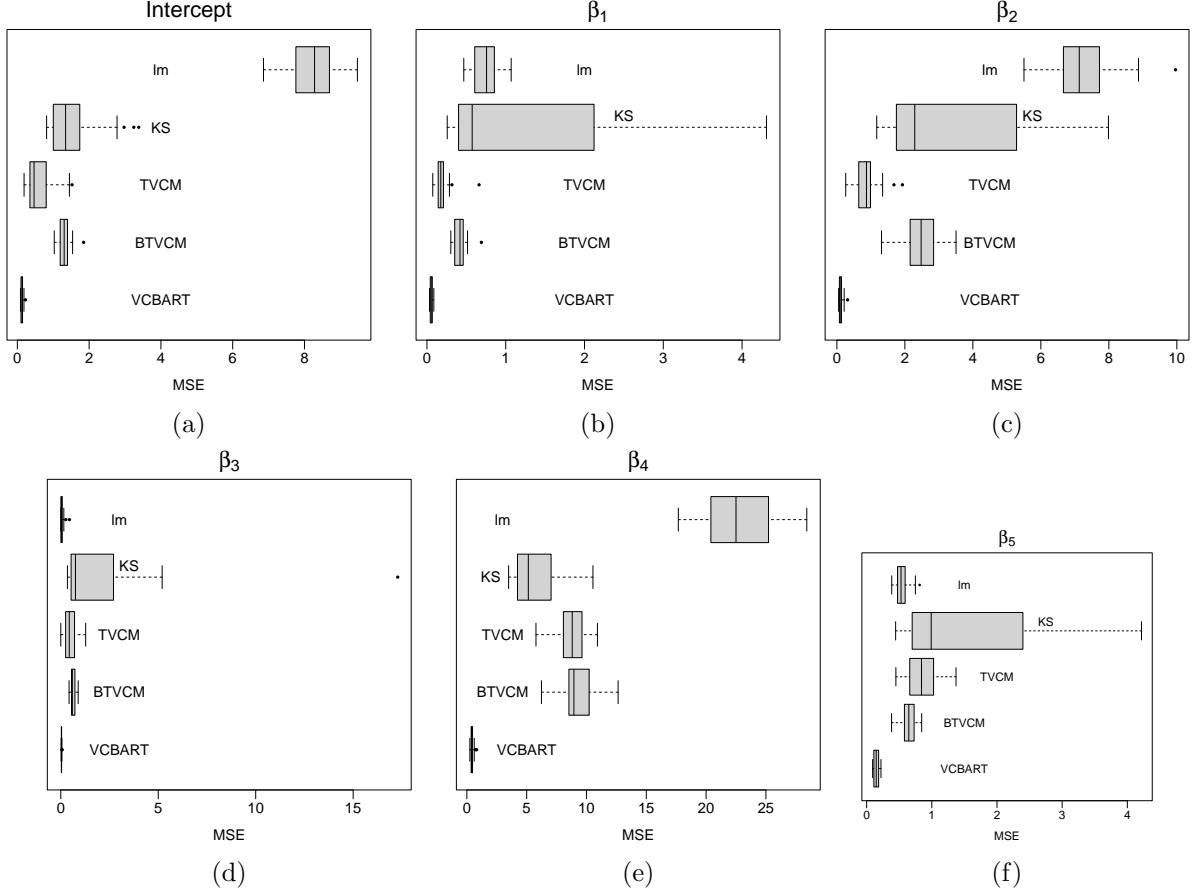


Figure S9: Analog of Figure 3a of the main text showing the out-of-sample mean square error for estimating each $\beta_j(z)$ in our main experiment function-by-function.

S3.3 Scalability and stability

Recall from Section 4 of the main text that we performed a second synthetic experiment to study VCBART's ability to scale to larger datasets. Like the main simulation study, we generated data from a varying coefficient model in which each of n subject contributed four observations. By varying N between 25 and 12,500, we were able to see how VCBART performed when trained on as few as 100 and as many 50,000 total observations. Like our main experiment, we simulated 4 MCMC chains for 2,000 iterations, discarding the first half of each chains as burn-in. Figure S11 plots the covariate effect estimation, uncertainty interval coverage, modifier selection, and runtime as functions of the total number of observations N .

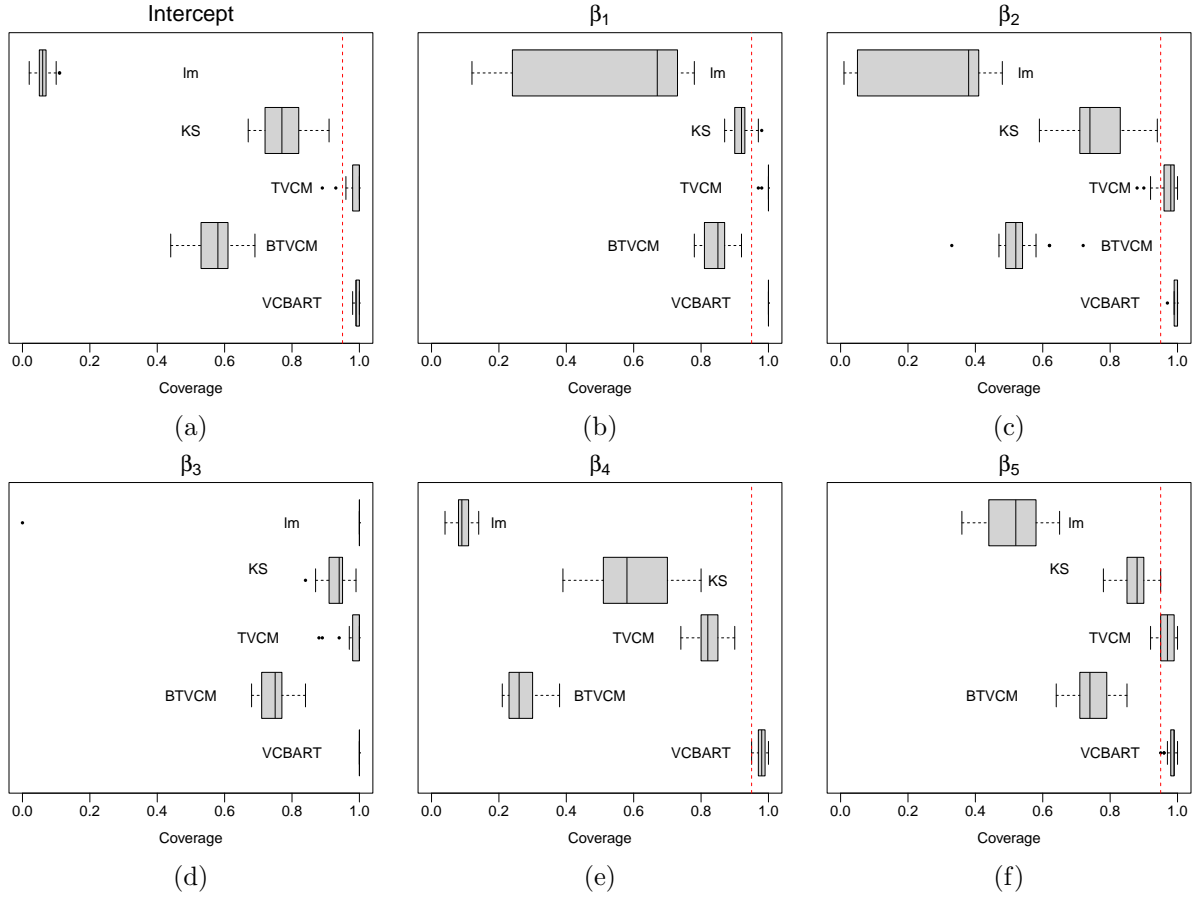


Figure S10: Analog of Figure 3b of the main text showing the coverage of the 95% credible intervals for estimating each $\beta_j(\mathbf{z})$ out-of-sample in our main experiment function-by-function.

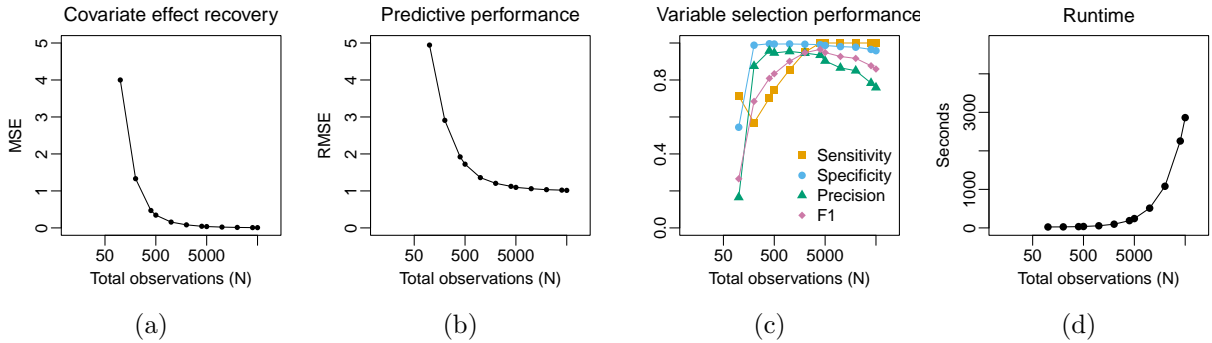


Figure S11: VCBART's estimation, prediction, and variable selection performance as a function of the total number of observations N . Average MSE for evaluating β_j 's (a) RMSE for predicting responses y (b), $F1$ score, precision, and sensitivity (c), and total time in seconds to run four chains sequentially (d). Note the log-scale on the horizontal axis